U.S. DEPARTMENT OF ENERGY

PNNL-20849

Prepared for the U.S. Department of Energy
under Contract DE-AC05-76RL01830

Requirements for Defining Utility Drive Cycles:

An Exploratory Analysis of Grid Frequency Regulation Data for Establishing Battery Performance Testing Standards

R Hafen
V Viswanathan
K Subbarao
M Kintner-Meyer

October 2011

Pacific Northwest
NATIONAL LABORATORY

Proudly Operated by Battelle *Since 1965*

DISCLAIMER

PACIFIC NORTHWEST NATIONAL LABORATORY
operated by
BATTELLE
for the
UNITED STATES DEPARTMENT OF ENERGY
under Contract DE-AC05-76RL01830

Printed in the United States of America

Available to DOE and DOE contractors from the
Office of Scientific and Technical Information,
P.O. Box 62, Oak Ridge, TN 37831-0062;
ph: (865) 576-8401
fax: (865) 576-5728
email: reports@adonis.osti.gov

Available to the public from the National Technical Information Service,
U.S. Department of Commerce, 5285 Port Royal Rd., Springfield, VA 22161
ph: (800) 553-6847
fax: (703) 605-6900
email: orders@ntis.fedworld.gov
online ordering: http://www.ntis.gov/ordering.htm

This document was printed on recycled paper.
(9/2003)

PNNL-20849

Requirements for Defining Utility Drive Cycles:

An Exploratory Analysis of Grid Frequency Regulation Data for Establishing Battery Performance Testing Standards

R Hafen
K Subbarao
V Viswanathan
M Kintner-Meyer

October 2011

Prepared for
the U.S. Department of Energy
under Contract DE-AC05-76RL01830

Funded by the Energy Storage Systems Program of
the U.S. Department of Energy

Pacific Northwest National Laboratory
Richland, Washington 99352

Abstract

Battery testing procedures are important for understanding battery performance, including degradation over the life of the battery. Standards are important to provide clear rules and uniformity to an industry. The work described in this report addresses the need for standard battery testing procedures that reflect real-world applications of energy storage systems to provide regulation services to grid operators. This work was motivated by the need to develop Vehicle-to-Grid (V2G) testing procedures, or V2G drive cycles. Likewise, the stationary energy storage community is equally interested in standardized testing protocols that reflect real-world grid applications for providing regulation services.

As the first of several steps toward standardizing battery testing cycles, this work focused on a statistical analysis of frequency regulation signals from the Pennsylvania-New Jersey-Maryland Interconnect with the goal to identify patterns in the regulation signal that would be representative of the entire signal as a typical regulation data set. Results from an extensive time-series analysis are discussed, and the results are explained from both the statistical and the battery-testing perspectives. The results then are interpreted in the context of defining a small set of V2G drive cycles for standardization, offering some recommendations for the next steps toward standardizing testing protocols.

Executive Summary

The work described in this report is of importance to the general energy storage community. The motivation for this analysis was inspired by the persistent interest in the Vehicle-to-Grid (V2G) concept, which is a strategy that requires a bi-directional exchange of electric energy with the electric grid and results in compensation of the owners of the vehicles by a grid operator. There is a rich body of literature with discussions about the value of V2G, and many universities and research organizations are involved in research focused on control strategies to optimize the battery management system and overall system performance. Despite this enthusiasm by the research community seeking to maximize the total value of a vehicle, the automotive manufacturing and transportation battery communities are reluctant to embrace V2G applications. This reluctance is based on a lack of knowledge about battery degradation associated with the exposure to grid applications.

This work addresses this knowledge gap. It initiates an effort toward standardizing a set of duty cycles for battery performance testing procedures that will be representative of real utility applications. The work described in this report focuses on the characterization of grid services. We envision that this and follow-on work will provide the basis for standards-development discussions that cover the entire spectrum of conditions that a battery may be exposed to during V2G applications. This work is equally important for stationary energy storage systems because industry is demanding definitions and standardization of performance testing procedures that represent typical utility duty cycles.

This report discusses the findings of a statistical analysis that utilized frequency regulation data from the Pennsylvania-New Jersey-Maryland Interconnect (PJM). A data set containing 4-second regulation data for a period of 175 days spanning from the time period March 2011 through August 2011 was processed. The objective of this work was to search for potential patterns or differentiations in the signal that would allow us to postulate one or more typical and distinct duty cycles or sequences of regulation segments that are representative for PJM's regulation services. It was unclear at the beginning of the study if a time-dependent parameterization would be possible. In other words, would the signal indicate a different characteristic as a function of time-of-day or even month-of-the-year? The results of a statistical exploration of the data set and our findings in the context of battery life impacts are summarized. We explored the possibility of defining a set of duty-cycle candidates that could be discussed with the broader energy storage community for initiating standards development activities.

The following synopsis provides an overview of the key outcomes of this work.

1. Spectral results

The spectral analysis revealed patterns in the regulation signal with distinct periodicities in the 1-hour, 30-minute, and 7.5-minute cycles. These periodicities are believed to reflect the specific PJM market design.

2. Time-of-day difference observations

- *Mean value of regulation:* There is a propensity for the mean of the regulation signal to be slightly biased above zero during the middle of the day (06:01 to 18:00) and slightly biased below zero during the night (18:01 to 06:00). This finding has important implications to batteries in

that, unless otherwise compensated, on average there would be a resulting net charge of a battery plugged in during the night and, conversely, a net discharge during the day. A net charge during the night for plug-in electric vehicles can be accommodated easily without any compensation, but a net discharge during the day will need to be compensated so the vehicle battery can be recharged for the next drive.

- *Amplitude of regulation cycling:* The amplitude swing (i.e., the minimum-maximum spread) of the cycles in the regulation signal has a propensity to be higher at night and lower during the day. In fact, we found that a significant relationship exists between the system load level and the amplitude of the regulation signal; that is, under low-load conditions, the amplitude of regulation grows exponentially compared regulation under high-load conditions. This means that, during the day, either fewer vehicle resources are necessary to meet the regulation requirements, or if the resource availability constant is kept constant during the 24-hour period (i.e., the same number of vehicles offering the same service for 24 hours), the individual contribution by each vehicle is less during the day than during the night. As a consequence, the amplitude for defining a performance test or drive-cycle could potentially be smaller during the day than at night.

3. Seasonal (month-of-the-year) differences observations

Exploring the range of low-frequency (1-hour cycles) to high-frequency (7.5-minute cycle) signals across all seasons indicates that the lower frequency component in the regulation signal increases in significance during winter to summer months. The mid-range frequency (30-minute cycle) remains constant over the months studied, while the higher-frequency components (7-minute cycle) slightly decrease their contribution to the overall signal from March through August. Low-frequency cycles require more energy (kWh) capacity than do high-frequency cycles. Low-frequency cycles with higher energy requirements cause large cycles across the state-of-charge (SOC) scale for any given battery size. For transportation batteries, this would place a higher burden on the remaining life of the battery, as it may encounter deeper depths of discharge over any given period of time than would occur if the battery was exposed to higher frequency regulation signals. This also could affect thermal management of batteries at low SOCs as the internal resistance is higher at low SOCs. Hence, in addition to energy considerations, the ability of the batteries to provide the required power at low SOCs needs to be assured as part of the test profiles being developed.

4. Other observations

- The statistical clustering approach used in this work reflected the large diversity in regulation signal patterns, thus resulting in rather large numbers of clusters to characterize the entire data set. As a consequence, the prospect of finding a small number of representative cycles solely derived from the clustering approach does not seem to be promising. Additional information based on an understanding of battery testing procedures must be used to inform the selection process.

- Despite of the large diversity in regulation data the analysis distinguished clusters of similar behavior based on dominant low-frequency cycles (30-minute to 1-hour cycles).

- Cycles in the same cluster have similar time-of-day properties, indicating similar patterns occur in many cases at the same time of the day.

- The regulation signals revealed system behaviors of PJM's market structure. The 1-hour cycle components of the regulation signal clearly reflect the hourly markets, thus causing a rearrangement of generators participating in the day-ahead hourly energy market. The regulation signal dependency on the frequency and timing of market clearings suggests that the results are strictly valid for the current PJM wholesale markets. As PJM's market design changes, it is very likely that the key oscillatory content also will change. With the general trend in the competitive wholesale market to clear in shorter and shorter time periods, there could be a propensity for regulation signals to increase the importance of the shorter cycles. Furthermore, integration of the increasing capacity of intermittent wind and solar resources will very likely introduce new dynamics to the regulation requirements caused by the varying output of the wind and solar installations. How the growing wind and solar capacity may influence the regulation signal is unclear. Weather phenomena and the diversity of the wind and solar insolation across a balancing area will impact the regulation signal. Furthermore, the change in the generation inertia by the growing wind and solar generation also may influence the dynamics of the power system and, in turn, impact the regulation signal.

5. Recommendations for selection of V2G drive cycles

Despite the large diversity of lower- and higher-frequency characteristics across the time scale in the PJM data set, we do offer some recommendations for the selection of potential candidates for testing cycles that is informed by battery experts. As a result, the recommendations are based on both the findings of the cluster analysis and then further informed by an understanding of battery degradation mechanisms and battery performance testing. From 30 distinct clusters, a set of duty cycles from three particular clusters are recommended as potential candidates for future standards development. They are discussed as follows:

1. *Curves with directionality and sign of the signal changing from positive to negative or vice versa*. Cluster 1 in Figure 3.6 is an example of a representative duty cycle for this characteristic.

2. *A low frequency signal*. Cluster 10 is an example.

3. *High frequency signals oscillating symmetrically around zero*. This case is quite straightforward and is ideal for batteries. Cluster 17 is an example.

6. Next Steps toward standardizing V2G drive cycles

This analysis is the first of several steps toward standardizing V2G drive cycles or battery testing cycles. The next step is to perform a similar exploratory analysis with regulation data sets from other regions of the United States to explore potential regional differences that are reflective of different market designs, system responses, and system characteristics. After these regional studies, the results can be discussed from a national perspective to identify a set of characteristics that are sufficiently representative of the U.S. grid.

It is anticipated that the statitistical analyses will provide the background information needed to formulate a set of test procedure proposals. With continuing support for this analysis, it is reasonable to expect statistical analysis for the entire United States could be completed toward the end of FY 2012, with standards discussions commencing in the fall and winter of 2012. The appropriate standards body would be the Institute of Electrical and Electronics Engineers.

Acknowledgments

The authors wish to thank Mr. Scott Baker and Mr. Ken Hubert from PJM for providing the data set and very valuable comments regarding this research, and Dr. Ning Lu from Pacific Northwest National Laboratory for her advice and interpretation of some of the electric power systems behavior observed in the data.

The authors also would like to thank Mr. Dan Ton of the U.S. Department of Energy, Office of Electricity Delivery and Energy Reliability for funding this work.

Acronyms and Abbreviations

CWT	continuous wavelet transform
DWT	discrete wavelet transform
PHEV	plug-in hybrid electric vehicle
SOC	state of charge
SOH	state of health
V2G	vehicle-to-grid
PJM	Pennsylvania-New Jersey-Maryland Interconnect

Contents

Abstract iii
Executive Summary iv
Acknowledgments vii
Acronyms and Abbreviations viii
1.0 Introduction 1
1.1 Motivation of Analysis 2
2.0 Exploratory Analysis 3
2.1 PJM Frequency Regulation Data 3
2.2 Systematic Mean Properties 4
2.2.1 Implication from a Battery Point of View 4
2.3 Systematic Variance and Amplitude Properties 5
2.3.1 Implication from a Battery Point of View 7
2.4 Scaling Signals 7
2.4.1 Scaling the Mean 7
2.4.2 Scaling the Variance and Amplitude 8
2.5 Spectral Properties 9
2.5.1 Implication from a Battery Point of View 10
2.6 Time-Scale Behavior 11
2.7 Within-Hour Variation 12
3.0 Determining Representative Drive Cycles 16
3.1 K-Centroids Clustering 16
3.1.1 Feature Vectors and Distance Metrics 17
3.2 Discrete Wavelet Transform 17
3.3 Wavelet Coefficients by Scale 19
3.4 Periodogram Features 20
3.5 Choosing the Number of Clusters 20
3.6 Evaluating Cluster Results 22
3.7 Choosing a Representative Signal 27
4.0 Conclusions and Future Work 28
4.1 Exploratory analysis results 28
4.2 Cluster Analysis 29
4.3 Recommendations for Selection of V2G Drive Cycles 29
4.4 Next Steps Toward Standardizing V2G Drive Cycles 30
5.0 References 31

Figures

Figure 1.1. Load Profile at Different Scales 1
Figure 2.1. Four Days of Arbitrarily Selected PJM Regulation Data 3
Figure 2.2. Means of 2-Hour Time Blocks against Time-of-Day across Month-of-Year 4
Figure 2.3. Amplitude of 2-Hour Blocks against Time-of-Day across Month-of-Year (differentiated by weekend and weekday) 6
Figure 2.4. Relationship of Peak-to-Peak Amplitude and Load 6
Figure 2.5. Battery Level from a Frequency Regulation Signal with and without Shifting the Mean 8
Figure 2.6. Example of Scaling a Frequency Regulation Signal 8
Figure 2.7. Two Scaled 2-Hour Samples with their Corresponding Periodograms 10
Figure 2.8. Boxplots of Periodogram Values vs. Month of Year across each Period 11
Figure 2.9. CWT for Two Different Signals (one from 00:00 to 02:00 and one from 18:00 to 20:00) 13
Figure 2.10. Example of Low-Pass Filter (blue) applied to a 2-Hour Block of Frequency Regulation Data 14
Figure 2.11. Low-Frequency Behavior by Hour-of-Day with Mean Behavior in Red 15
Figure 3.1. Discrete Wavelet Transform for a 2-Hour Period of Frequency Regulation Data 18
Figure 3.2. Original Frequency Regulation Data with Inverse DWT of Threshold Coefficients 19
Figure 3.3. Cluster Sums of Squares for Different Choices of *K* 21
Figure 3.4. Image Plot of Cluster Segments Overlaid by Neighborhood Graph of Wavelet Coefficient Clustering 22
Figure 3.5. Boxplot of Coefficients within Clusters 6, 15, and 19 23
Figure 3.6. All Series in Each of the 30 Cluster Signals Overplotted 24
Figure 3.7. Time-of-Day Plot 26

1.0 Introduction

Power system operators continuously balance generation and load. The load can be decomposed into base-load, load-following, and regulation components. The blue line in Figure 1.1 shows the sum of the base-load and load-following components [6]. The green line shows the actual load, and the difference between the green and the blue lines represents regulation as shown on an expanded scale by the red line.

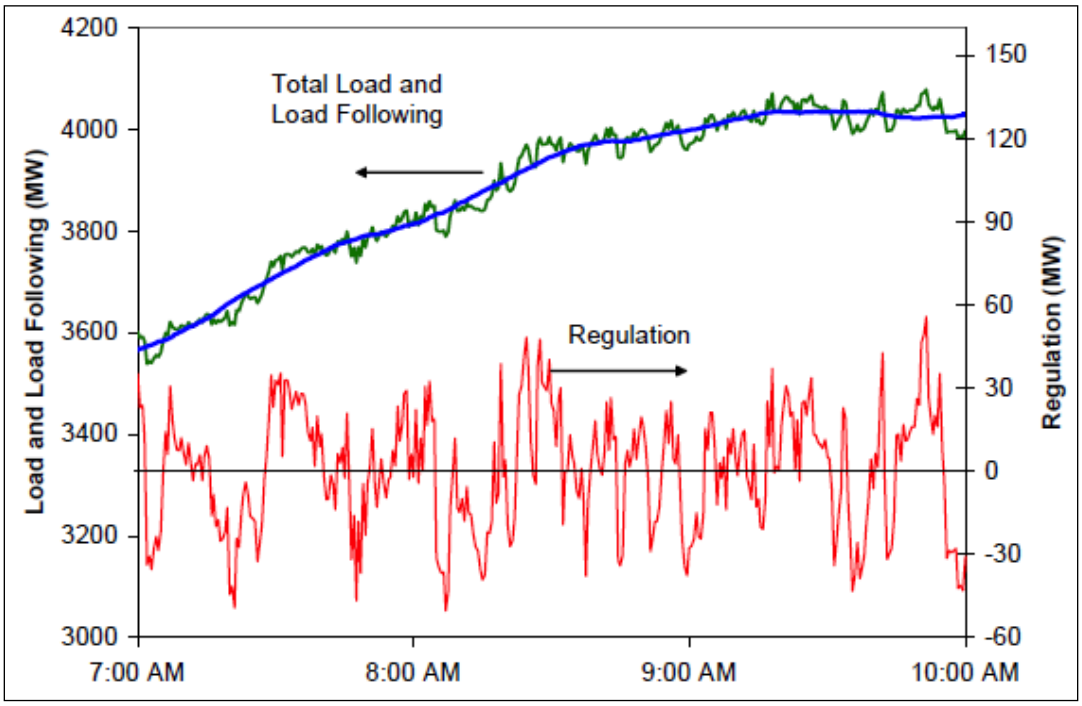

Figure 1.1. Load Profile at Different Scales

Load following represents the general trend over a time scale on the order of 10 minutes, whereas regulation represents variations over a time scale on the order of 1 minute. Regulation requires online power sources under automatic generation control (AGC) that can provide rapid response to up and down requirements to correct for load fluctuations and unintended or unpredictable fluctuations in generator output.

Electric batteries are excellent candidates as regulation providers because of their quick response and precise control. Both stationary batteries and batteries in plug-in electric vehicles (PEV) can provide regulation services. It is of utmost importance to both the stationary energy storage and the transporation battery industries to understand the use patterns for typical or representative real-world regulation service duty cycles. To provide insights into the characteristics of regulation signals, this analysis was initiated as a starting point. This report discusses the results from a statistical analysis of one set of data from the Pennsylvania-New Jersey-Maryland Interconnect (PJM). It explains the results from a statistical perspective and then projects the results into a battery context. Throughout this work, a set of statistical tools was developed that would allow analysts to process regulation signals from other grid operators to explore regional variations in the statistics of regulation data.

1.1 Motivation of Analysis

The analysis of regulation data is of importance to the energy storage community at large. The actual motivation for such analysis first emerged during the hightened interest in Vehicle-to-Grid (V2G) applications as a means to provide regulation service to grid operators. There is a rich body of literature that focuses on the value of V2G, and many universities are involved in research of control strategies to optimize the battery management system and overall system performance. Despite this enthusiasm by the research community seeking to maximize the total value of a vehicle by exploring other services beyond the transportation, the automotive manufacturing and transportation battery communities remain reluctant to embrace V2G applications because of uncertainties associated with the exposure to grid applications and concerns about potential degradation of the transportation battery. Rather than to delving into another technology demonstration to test the degradation of transportation batteries during mixed use (for its primary use of transportation and its secondary use as a grid service provider), we initiated a statistical analysis with the goal of characterizing one or more typical V2G profiles that then could be standardized as a V2G- or utility-drive profile, very similar to the other vehicle drive cycles that represent typical driving behaviors (such as Federal Test Procedure 75 [4]). The goal is to indentify if there are regional differences or temporal differences that would require several standard test cycles representative for the entireV2G application spectrum.

During the early phases of this work, we realized that the need to characterize regulation data is not only a concern for the transportation battery industry but likewise for the stationary energy storage community. As the stationary storage community is gaining momentum, battery vendors are seeking standards against which they can test their energy storage products. There now is equal interest in standardizing various standards for stationary system to represent various duty cycles to which a modern battery could be exposed. The analysis undertaken in this study is the first step toward standardizing *duty cycles* (the term commonly used for the storage energy storage community) or *drive cycles* (the term commonly used in the vehicle community).

2.0 Exploratory Analysis

This section presents the results of an intensive exploratory data analysis of frequency regulation data. The purpose of this analysis is to uncover any information that reveals insights into the nature of the regulation signal and how it behaves with regard to known physical factors such as time-of-day or time-of-year. Regulation patterns are interesting in that they exhibit both random and deterministic behavior. The signal is fundamentally driven by load, which in the short term is very stochastic in nature. We presume that there are different patterns in the regulation signal due to the time-of-day and the time-of-year because of how human activity changes throughout the course of the day and year, and possibly because of the inertia in the entire grid that changes with the level of generation and the generation mix.

2.1 PJM Frequency Regulation Data

The signal of interest in our study is the frequency-only regulation signal reported by PJM.

PJM has made regulation data publicly available for download from their website. At the time of this study, data was available continuously from March 2011 to August 2011. We studied 175 complete days of data,which amounted to approximately 3.8 million observations. The frequency regulation signal is time stamped and reported every 4 seconds. When studying time-of-day behavior, we honor daylight savings time because human activity ultimately drives the systematic variability in the data.

Figure 2.1 illustrates what the frequency regulation signal looks like for four randomly sampled days. The data fluctuates around zero in cycles. In this figure, we see that properties of the signal can vary from one day to the next and across the course of a day. For example, the cycles on April 17 have quite a high amplitude throughout the course of the day when compared to June 10. There seems to be a pattern of higher amplitudes during the midnight hours in each day. These and many more observations are discussed in greater detail in the following sections.

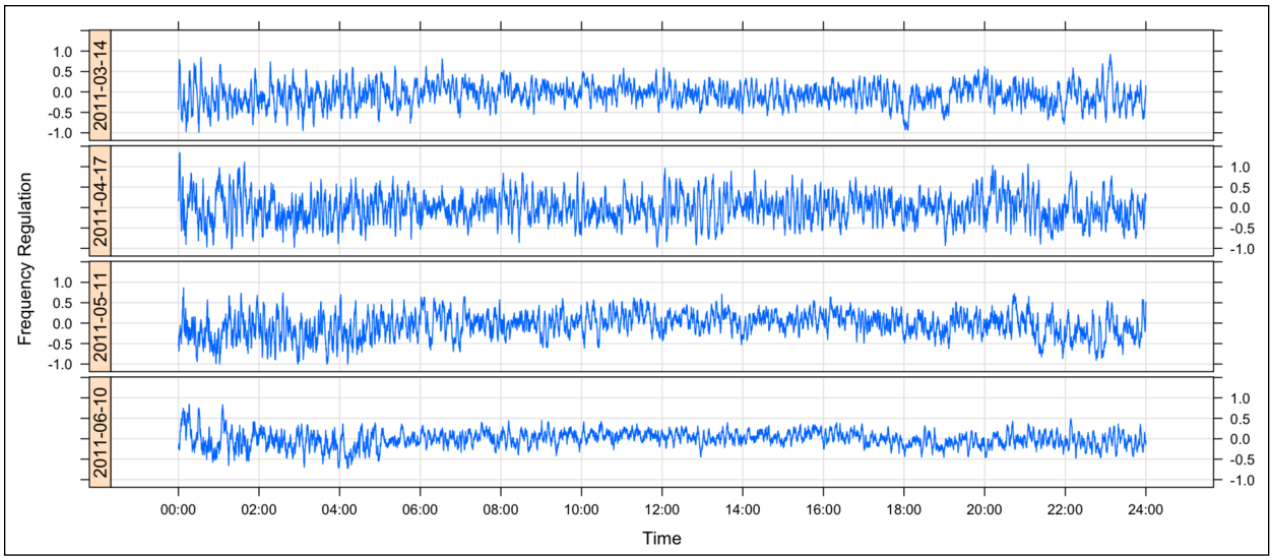

Figure 2.1. Four Days of Arbitrarily Selected PJM Regulation Data

2.2 Systematic Mean Properties

From Figure 2.1, we have some reason to investigate the properties of the low-frequency mean behavior of the data over time because it appears to stray slightly from zero at times. For example, the early morning hours of May 11 are consistently below zero. Here we investigate whether there is any systematic behavior in the low-frequency means. To do so, we split the data into 2-hour blocks, with 1800 observations within each block. Let $x_1^{(d,h)}, \ldots, x_n^{(d,h)}$ denote the series of observations for day $d, d = 1, \ldots, 175$ beginning at hour $h, h = 0, 2, 4, \ldots, 22$, with $n = 1800$. We simply compute the sample mean within each block $\bar{x}^{(d,h)} = 1/n \sum_{i-1}^{n} x_i^{(d,h)}$ and group them by time-of-day.

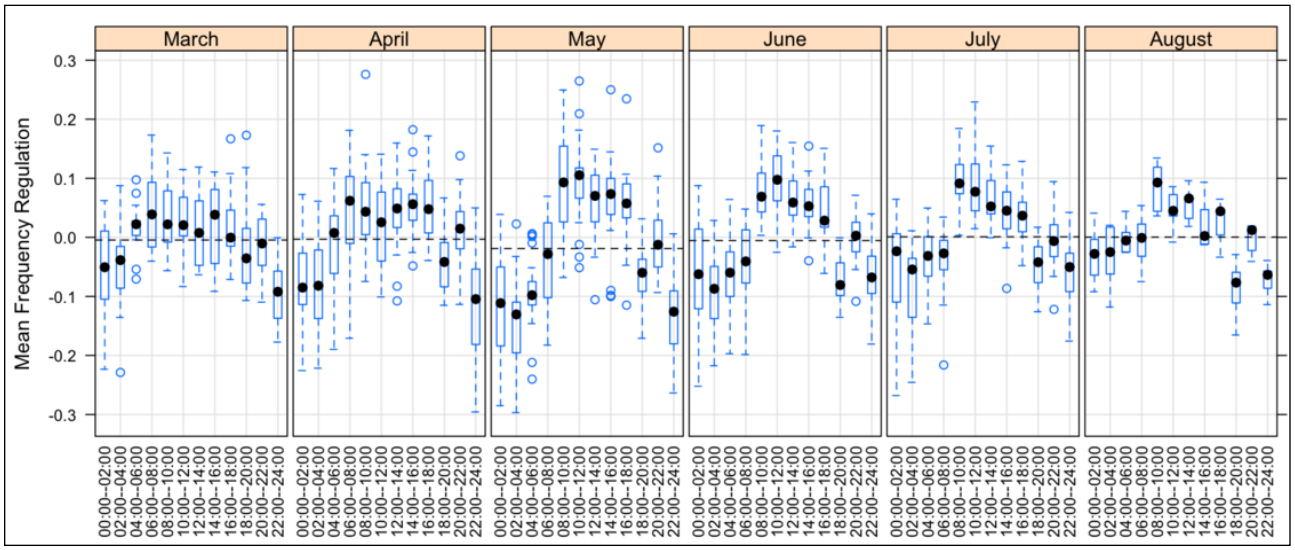

Figure 2.2. Means of 2-Hour Time Blocks against Time-of-Day across Month-of-Year

Figure 2.2 shows boxplots of the means against time-of-day across months. This plot allows us to directly compare the median, indicated by a filled black dot, and the 25th and 75th quantiles, which determines the range of the box across the time-of-day and time-of-year. A very consistent pattern emerges. While the range of the means is quite large within each boxplot (illustrated by the dashed lines extending from the box), we see that the frequency regulation signal is typically negatively biased during the night-time hours and slightly positively biased during the middle of the day, and that this pattern is consistent across time-of-year.

2.2.1 Implication from a Battery Point of View

This finding has important implications on a battery providing regulation service based in this signal. Before explaning these, we first point out that a positive frequency regulation signal means that a battery providing regulation service must inject electricity into the grid (i.e. discharge) while a negative frequency regulation signal means that a battery must withdraw energy out of the grid (i.e. charge).

Time-of-day differences are noticeable in the statistical means of the regulation signal. The propensity for the means to be slightly negative at night and slightly positive during the day for all months suggests that, on average, the regulation signal demanded more decrementing the generation

during the night and incrementing during the day. From a battery perspective, this means that, on average, there would be a resulting net charging during the night and, conversely a net discharging during the day. This means that the cycling would be a slight charging trend during the night, while during the day, the trend would drift to a slight discharging trend. To put this into the perspective from a transportation battery, the slight charging trend could be easily accommodated, because on net, the vehicle battery would need to be recharged at night anyway. The slight charging trend would cause the battery to be charged slightly sooner than otherwise predicted.

To provide the regulation service during the day, the slight discharging trend most likely will need to be compensated by the vehicle battery management system by resetting the operating point around which the battery performs charging/discharging cycles. In most cases, for V2G applications during the day, the battery management system would perform some biasing (i.e., moving the average operating point) upward so the vehicle battery will be on a net recharge trend. This would ensure that the battery will never be depleted by V2G applications during the day; rather, it would be partially or fully recharged by a given time.

2.3 Systematic Variance and Amplitude Properties

There are many interesting properties related to the magnitude of the cycles of the frequency regulation data. A classical statistical measure of variability is the variance, which measures the deviation of the series from the mean. Another measure more suited to cyclical data is the amplitude. We continue operating in 2-hour time blocks; however, in this section, for a given day and 2-hour block, we replace $x_i^{(d,h)}$ with x_i to simplify the notation. The sample variance in each block is calculated as $\hat{\sigma}^2 = 1/(n-1)\sum_{i=1}^{n}(x_i - \bar{x})^2$. The sample standard deviation $\hat{\sigma}$ is simply the sample square root of the variance. While amplitude can be measured in different ways, here we define the maximal amplitude within a 2-hour block as the maximum absolute value in the block, $A = \max|x_i|$. For this data, we made a comparison of the standard deviation and the maximal amplitude and found them to be extremely similar. Figure 2.3 is a plot of the maximal amplitude within each 2-hour block plotted against time-of-day across time-of-year.

In this figure, we plot the raw data rather than boxplots, so that we can visually compare the amplitute on weekends versus weekdays. A smooth line is plotted through each panel for weekday/weekend, highlighting the mean of the values across the course of the day. The hour-of-day variables are "jittered", by adding a small amount random noise to avoid overplotting. There are some very striking features in this plot. First, we confirm our suspicion that the amplitude of the frequency response signal is greater during the midnight hours, and decreases in the middle of the day. Also, we see that the amplitude is decreases from one month to the next. We also see that there are slight differences between weekends and weekdays that appear to be significantly different at many points, especially in May.

These results led us to hypothesize that the amplitude of the frequency regulation signal is higher when the load is lower. To support this, consider how the amplitude is highest during the night-time, during the weekends, and during the pre-summer months, which are times when the load is lowest. To investigate this relationship, we obtained hourly load data for PJM and compared the average load during each 2-hour period to the corresponding 2-hour maximal amplitude value. Figure 2.4 shows a plot of the frequency regulation amplitude versus the corresponding load calculated at each 2-hour block. The second plot shows each variable on the log scale. This plot clearly indicates a fairly strong relationship

between the amplitude of the frequency regulation signal and the load. The solid black line overplotted is the fitted line according to the relationship described below.

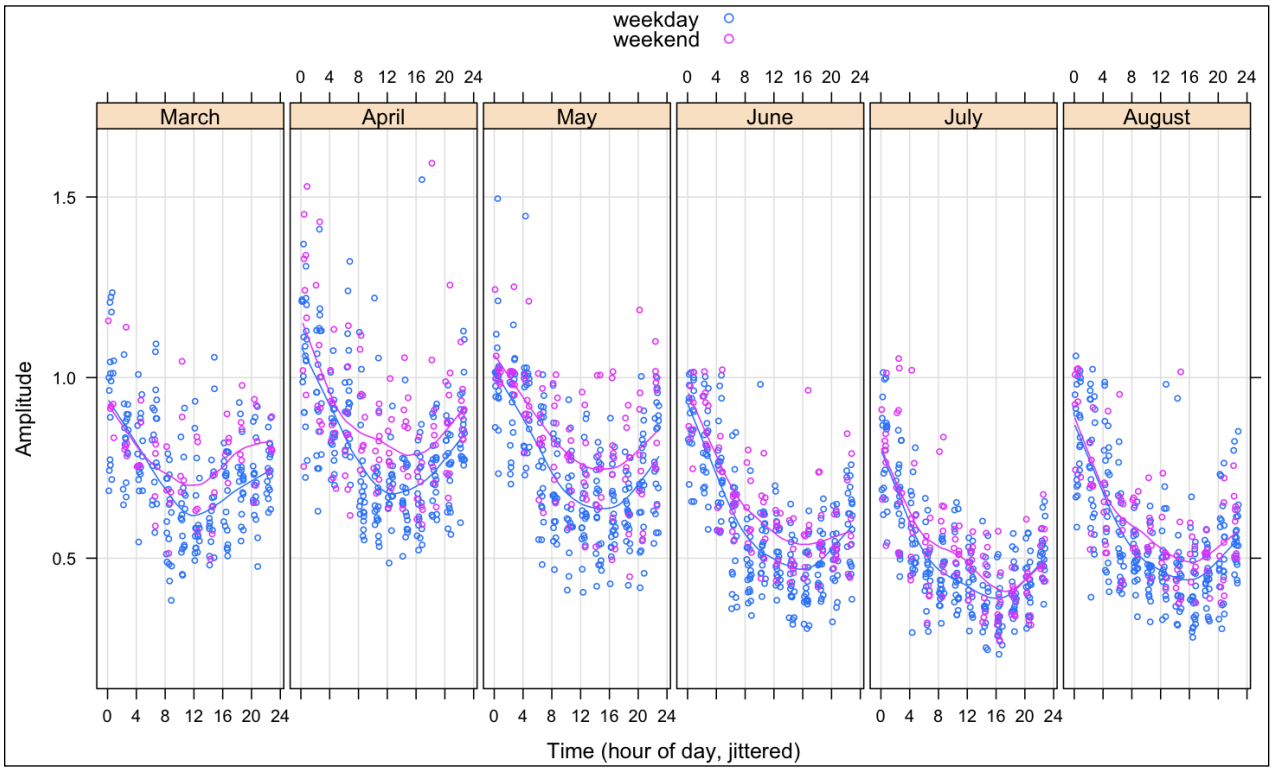

Figure 2.3. Amplitude of 2-Hour Blocks against Time-of-Day across Month-of-Year (differentiated by weekend and weekday)

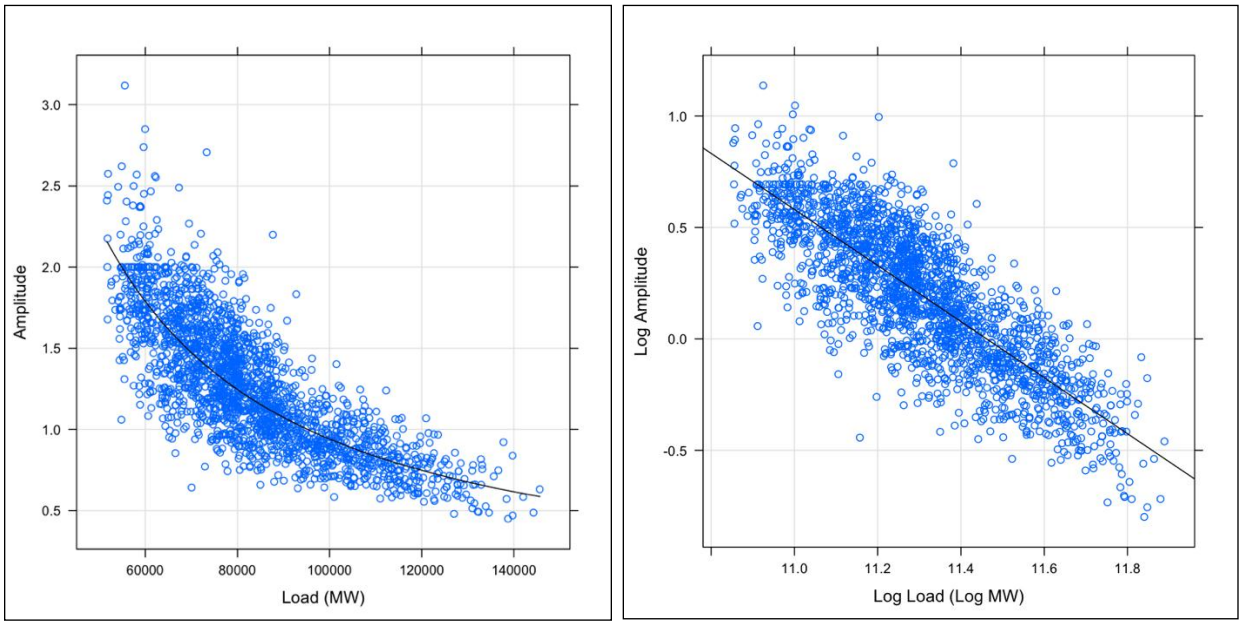

Figure 2.4. Relationship of Peak-to-Peak Amplitude and Load

The log-log linear relationship is indicative of a power law, so that the amplitude has the following relationship with load:

$$amplitude \approx \alpha(\, load\,)^{\beta}.$$

This relationship can be very useful in determining how many batteries need to be be plugged in given the load level.

2.3.1 Implication from a Battery Point of View

The exponential amplitude dependency on the load suggests that, during the day, either fewer vehicle resources are needed to meet the regulation requirements (fewer vehicles need to be engaged in V2G applications), or if we keep the resource availability constant during the 24-hour day (i.e., same amount of vehicles offering up the same service for 24 hours), the individual contribution by each vehicle is less during the day than at night. As a consequence, the amplitude for defining a test or drive-cycle could potentially be smaller during the day than at night.

2.4 Scaling Signals

Scaling a signal is a useful technique for removing certain trends that may mask subtle patterns in the signal. In preparation for the ensuring cluster analysis, we will apply scaling techniques to create comparable 2-hour data segments.

Furthermore, scaling is an important subject for the implementation of V2G or stationary storage applications. Because of the diversity in the sizes and in the state-of-charge (SOC) of expected transportation and stationary batteries, the duty cycle of an individual battery will most likely be scaled to match the total power rating and to accommodate the different SOC at the onset of the regulation service.

2.4.1 Scaling the Mean

If the frequency regulation signal is biased above or below zero, the battery will have a net discharge or charge. Figure 2.5 shows a plot of a 2-hour frequency regulation signal that is very slightly biased negatively (dashed line in first panel represents the mean), along with a plot of what the battery level would be (arbitrarily starting at zero) with and without shifting the mean of the signal to zero. If N batteries are plugged in, the effect of the net charge for an individual battery would be decreased by a factor of N, as each battery would incur a loss that, in aggregate, is equal to what is plotted. During the 2-hour regulation, the battery SOC is calculated to be the integral of the frequency regulation signal times a scaling constant. For this specific case, the battery SOC increases during this 2-hour period.

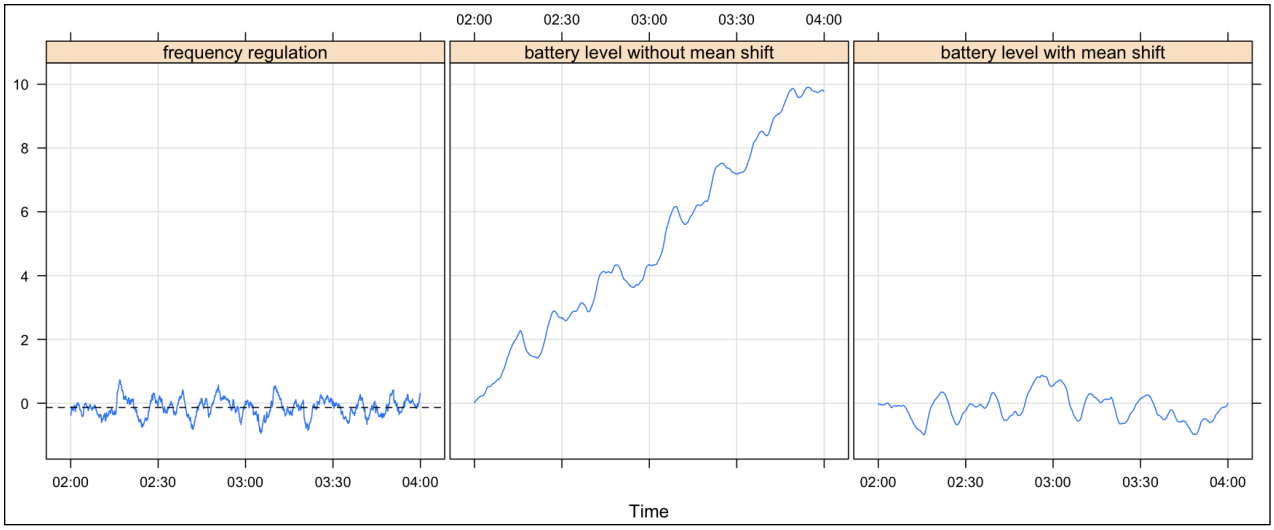

Figure 2.5. Battery Level from a Frequency Regulation Signal with and without Shifting the Mean

2.4.2 Scaling the Variance and Amplitude

A battery attached to the grid should have a set SOC range that it is not allowed to exceed. The bias of the frequency regulation signal determines the net charge/discharge that the battery is subjected to, hence its SOC, while the amplitude of the signal determines the power. In this study, we assumed that, within the SOC range investigated, the battery can provide the needed power during regulation. In reality, protocols described in the *PHEV Battery Test Manual* (plug-in hybrid electric vehicles [5]) should be used to estimate maximum power capability during charge and discharge of the battery.

To scale the amplitde, we scale each 2-hour block to a mean of zero, and then calculate the maximum absolute value. Then, we divide every value in the series by this maximum so the maximum value of the series does not exceed positive or negative one.

Figure 2.6 below illustrates the scaling method described for a 2-hour frequency regulation signal.

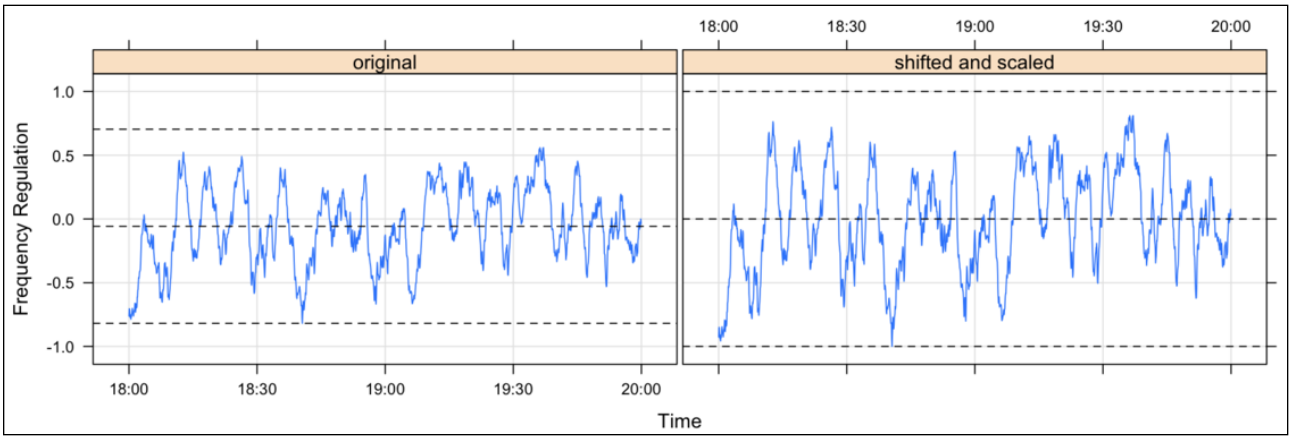

Figure 2.6. Example of Scaling a Frequency Regulation Signal

This transformed signal will be discussed in Section 2.5 and will be the basis for clustering methods described in Section 3.

2.5 Spectral Properties

An interesting variance property to investigate for the scaled regulation signal is the variance resulting from cyclical behavior at different frequencies. With $f_j = j/n, j = 1, \ldots, n/2$ as the *fundamental frequencies*, we can express the value of the frequency regulation signal through a spectral representation as a linear combination of sinusoids at various frequencies:

$$x_t = A_0 + \sum_{i=1}^{n/2} [\mathrm{A_j} \cos(2\pi f_j t) + B_j \sin(2\pi f_j t)]$$

The *periodogram* is an estimate of the spectral density of a signal and is calculated based on the $\mathrm{A_j}$ and $\mathrm{B_j}$ coefficients [3]. It provides a measure of the relative strength of cosine-sine pairs at various frequencies in the overall behavior of the series. The periodogram I at frequency f_j is:

$$I(f_j) = \frac{n}{2}\left(\hat{A}_j^2 + \hat{B}_j^2\right)$$

where

$$\hat{A}_j = \frac{2}{n}\sum_{i=1}^{n} x_i \cos(2\pi ij/n) \quad and \quad \hat{B}_j = \frac{2}{n}\sum_{i=1}^{n} x_i \sin(2\pi ij/n)$$

The periodogram at f_j is proportional to the sum of squares of the regression coefficients associated with frequency f_j, and hence is a measure of variability in the data at the given frequency. The plot below shows two scaled 2-hour samples with their corresponding periodogram. We slightly undersampled the data to get periodogram estimates at "nice" frequencies.

In Figure 2.7, we purposely chose two very different series in terms of periodic variance to highlight differences. The frequency on the x-axis is expressed in terms of cycles per 5 seconds, and values beyond frequency of 0.025 are not displayed because of the lack of any interesting data. In the periodogram plots, there are vertical gray lines corresponding to particular frequencies of interest, and the corresponding period for each of these frequencies is labeled. Many 2-hour blocks exhibit behaviors more like that of sample 1, with most of the energy due to 7.5-minute periodic behavior.

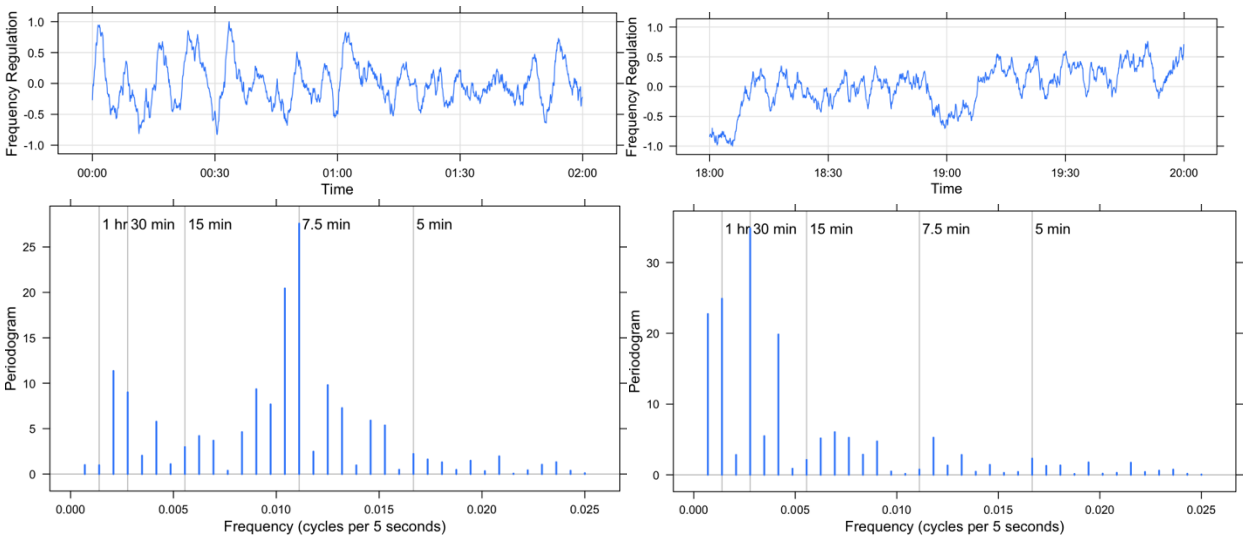

Figure 2.7. Two Scaled 2-Hour Samples with their Corresponding Periodograms

We conducted several explorations of the properties of these periodic variances. We found the variance resulting from any given period does not seem to change much across the time-of-day relative to the total variance. One interesting result, however, is related to how the periodogram values, or variance at each frequency, changes across the course of the year. Figure 2.8 plots the periodogram of the scaled signal at each frequency (translated to period in the labels) across time.

Low-frequency behavior is becoming more relatively dominant as time goes on, and periodic behavior of 8 minute periodicity and lower is increasing as time goes on.

Figure 2.8 clearly indicates a dependency of the frequency components of the signal as a function of month-of-the-year. Low-frequency behavior becomes more dominant from March to August, while high-frequency behavior becomes less important across the same time period.

2.5.1 Implication from a Battery Point of View

Low-frequency cycles require more energy (kWh) capacity than do high-frequency cycles. Put in a context of SOC, low-frequency cycles with higher energy requirements cause large cycles across the SOC scale of any given battery size. For transportation batteries, this means higher burden on the remaining life of the battery as it may encounter deeper discharge depths of over any given period of time than would occur if it was exposed to higher frequency regulation signals. The statistical implications are that there is a propensity for larger discharge depths in the signal in the summer months (July and August) than for the spring months (March and April).

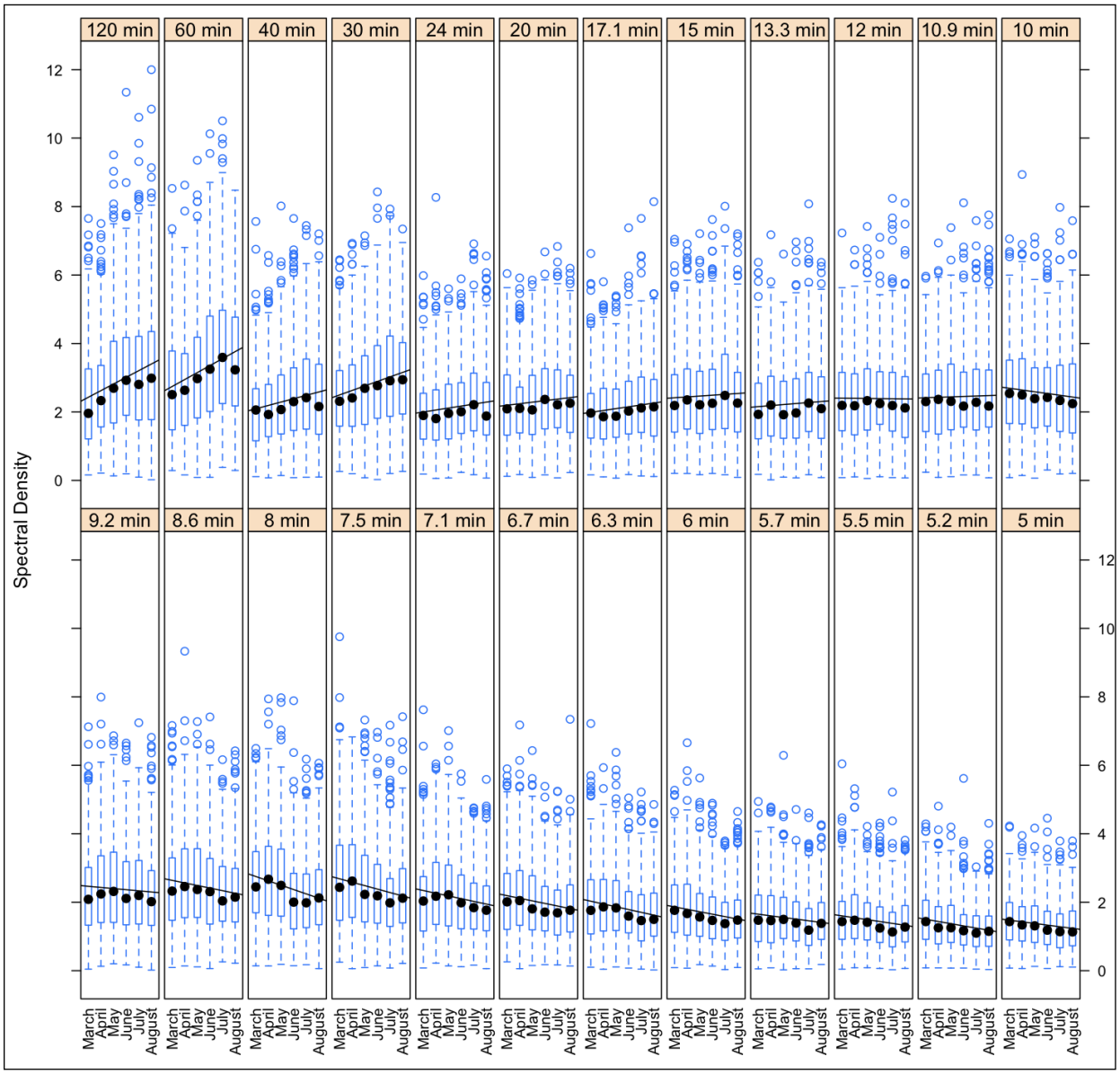

Figure 2.8. Boxplots of Periodogram Values vs. Month of Year across each Period

2.6 Time-Scale Behavior

Spectral methods, such as the periodogram discussed previously, are useful for understanding frequency behavior of time series. It is also useful to be able to understand how the frequency behavior of a series behaves over time. Spectral methods such as the short-term Fourier transform can be useful, but a more effective way to simultaneously view continuous time-scale information is through the continuous wavelet transform (CWT). The CWT is obtained through scaling and translating a mother wavelet, ψ to obtain:

$$\psi_{a,\tau}(t) = \frac{1}{\sqrt{a}}\psi\left(\frac{t-\tau}{a}\right),$$

where a is the scaling factor and τ is the shift parameter. The mother wavelet must satisfy various conditions. For a function x, the continuous wavelet transform is defined as

$$W_x(a,\tau) = \int_{-\infty}^{\infty} x(t)\psi^*_{a,\tau}(t)dt,$$

where * represents the operation of complex conjugate.

Wavelet methods are useful in that they do a nice job with the trade-off between time and frequency resolution, providing more resolution at higher frequencies and less resolution at lower frequencies.

In Figure 2.9, we plot the continuous wavelet transform using the second derivative Gaussian mother wavelet. The x-axis is time, and the y-axis is period (in minutes). The two plots correspond to the two frequency regulation series shown in Figure 2.7. Interesting features in these plots include the recurring 5- and 7.5-minute periodic behavior. The differences in the two series are clearly shown in the CWT plots, with the much stronger lower periodic behavior fot the second series.

The CWT plots were made for all 175 days and a qualitative comparision was made from one day to the next in hope of finding intereting patterns. Several patterns emerged, although they were not always consistent. One common pattern was an interesting lower frequency behavior happening around 18:00 (one example of which is the bottom CWT plot in Figure 2.9).

Just as in Figure 2.7, Figure 2.9 also indicates that the low-frequency contribution is dominant for the 18:00 to 20:00 time frame. This type of behavior was somewhat consistent when looking at the CWT plots for all days. As long as the battery SOC does not breach the design limits, this does not appear to be a roadblock to regulation.

2.7 Within-Hour Variation

All previous exploratory analysis has been done using computations based on 2-hour blocks of data. As a final part of our exploratory analysis, we explore how the mean and variance of the frequency regulation signal vary within each hour. While we do not leverage these results in our current analysis, we find the results interesting and feel that they will be of use in future modifications of our methodology.

To study the within-hour mean behavior of the frequency regulation signal, we wanted to ignore the higher frequency behavior, such as 7.5-minute cycles, and focus more on the lower frequency behavior. While we have shown that the grand mean for many 2-hour blocks of data varies from zero, we are interested in whether that variation from zero is constant or fluctuating. To investigate this, we applied a low-pass loess filter [2] with a moving window span of 17 minutes. Loess smoothing simply applies a local weighted polynomial regression sliding across time, and can be thought of as a low-pass filter. An example of such a filter applied to one hour of data is shown in Figure 2.10, with the loess smooth in blue. This filter highlights the slowly changing mean from positive to negative across the course of the hour.

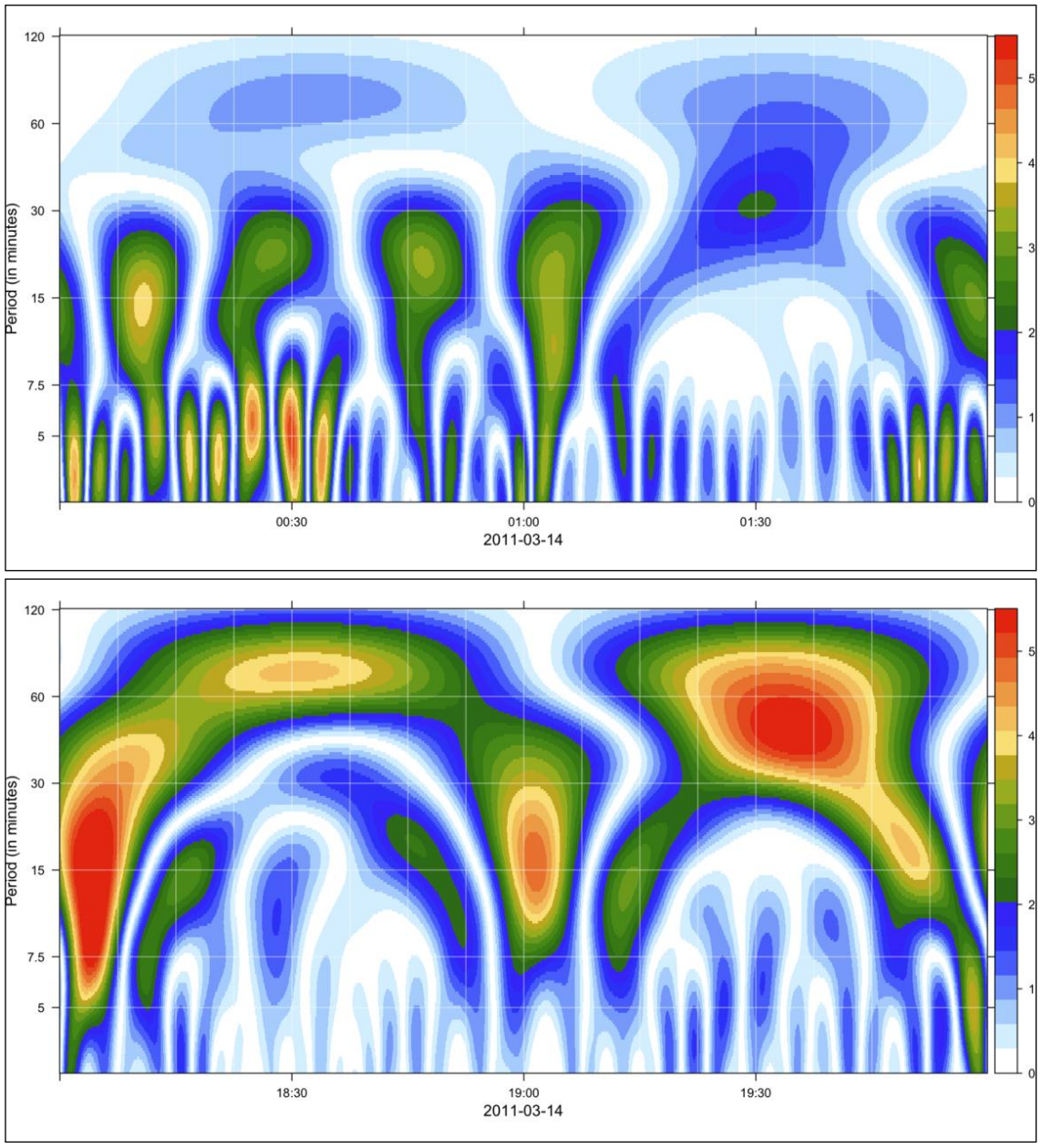

Figure 2.9. CWT for Two Different Signals (one from 00:00 to 02:00 and one from 18:00 to 20:00)

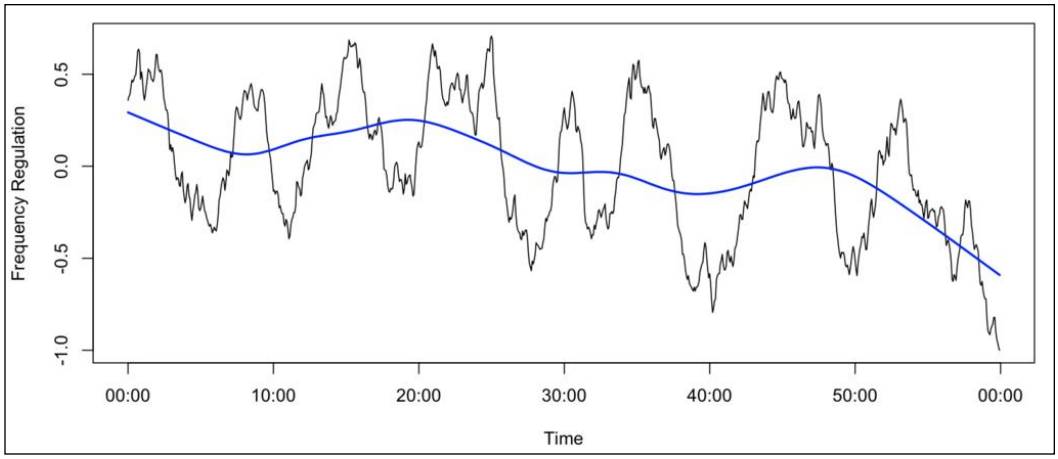

Figure 2.10. Example of Low-Pass Filter (blue) applied to a 2-Hour Block of Frequency Regulation Data

We applied this low-pass filter across the entire data set and examined it for characteristic patterns by time-of-day.

To study how the variance changes within each hour, we applied loess smoothing with a 37-minute moving window to the squared frequency regulation signal. This gives an estimate of the variance locally in time across the signal.

Figure 2.11 shows the smoothed local mean (top) and variance (bottom) values overplotted by time of day. The red line represents the average behavior of all the data at each point in time. Both plots verify what we have already seen, namely that the mean is higher during the middle of the day and lower during the night hours, and vice-versa for the variance. However, we get much more information because we see what is happening within each hour.

From 09:00 to 19:00, the mean behavior tends to droop at the beginning and end of each hour. There is very interesting up-down behavior during the midnight hours, and the humps in the middle of the hour at 05:00 and 06:00 are also interesting. There also are some interesting intra-hour dips in the variance plot during the off-peak hours.

What we learn from these plots is very useful in that it shows that there is systematic variation within each hour. Each individual series plotted in black varies considerably around the mean plotted in red, but there is a systematic pattern within each hour. In terms of using this information to help determine drive cycles, an initial clustering of low-frequency behavior followed by a study of the remaining signal with the low-frequency component removed might be worthy of consideration. Perhaps this knowledge can even be synthesized to generate guidelines for the construction of drive cycles and circumvent the need for clustering.

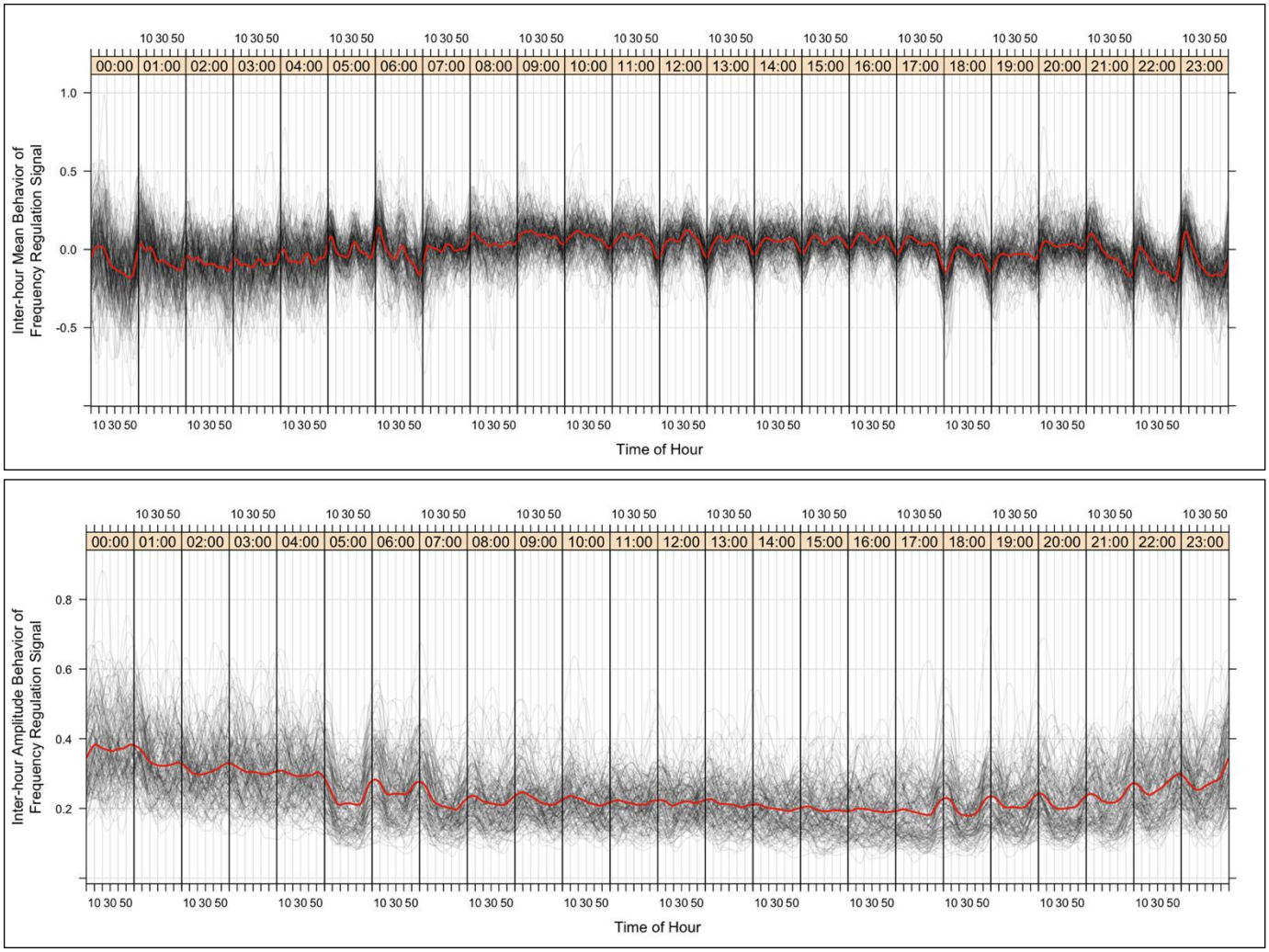

Figure 2.11. Low-Frequency Behavior by Hour-of-Day with Mean Behavior in Red

3.0 Determining Representative Drive Cycles

The exploratory analysis thus far has given some interesting insights into the behavior of the frequency regulation signal. This information can be used to guide understanding all the possible scenarios a battery following the signal can be exposed to. However, this may not be enough. For testing purposes, batteries need to be run through actual scenarios.

The goal of this section is to use unsupervised learning techniques to examine the data and find similar patterns that appear repeatedly in the data. The hope is that a handful of battery drive cycle tests will emerge based on this analysis. Our exploratory analysis cast some doubt on the existence of a small set of representative signals as we saw that even low-frequency behavior is quite variable (Section 2.7).

All our computation work was done using the R statistical environment [11]. Cluster analysis was done using the flexclust package [7].

3.1 K-Centroids Clustering

Given a set of feature vectors $(\mathbf{x}_1, \ldots, \mathbf{x}_n)$, where each observation $\mathbf{x}_i$ is a d-dimensional vector, the goal of K-centroids clustering is to partition the n observations into K sets, $S_1, \ldots, S_K$. The goal is to find a set of centroids $\mathbf{c}_1, \ldots, \mathbf{c}_K$ for which the average distance from each point to the closest centroid is minimal.

The general K-centroids clustering method is as follows:

- Start with a set of K initial cluster centroids, $\mathbf{c}_1, \ldots, \mathbf{c}_K$. These are typically K randomly chosen observations from the data.

Assign each point $\mathbf{x}_i$ to the nearest centroid, using a distance metric $D_{ij}(\mathbf{x}_i, \mathbf{c}_j)$, so that observation $\mathbf{x}_i$ is assigned to cluster set S_j if it is closer to centroid $\mathbf{c}_j$ than any of the other centroids.

For all observations in each set S_i, calculate the new centroid $\mathbf{c}_i$.

Repeate steps 2 and 3 until convergence is achieved.

In our setting, the goal is to see if there are meaningful clusters of the frequency regulation signal. The hope is that a good clustering will result in tight clusters of similar behavior, so we can provide recommendations for battery drive cycle tests based on these representative signals. Throughout this section, we will continue operating on 2-hour blocks of time as one observation. Thus, with this data set, we have 2100 observations.

There are many choices for feature vectors and for distance metrics. The well-known traditional K-means algorithm uses Euclidian distance and the mean centroid. To obtain good clustering, we must consider several possibilities with regard to which feature vector and which distance metric we will use.

3.1.1 Feature Vectors and Distance Metrics

The goal of a good feature vector is to express all of the relevant information about an observation while having low dimensionality. The most trivial feature vector in our setting would be the set of 1800 raw signal values within each 2-hour block. Other representations we consider here include the discrete wavelet representation of the series (discussed in the next section), the periodogram, and a condensed version of the periodogram.

With regard to the distance metric, we stick mostly with Euclidian distance. When using the periodograms as feature vectors, we also consider the earth mover's distance [9], which is useful for comparing probability distributions and calculates the cost of turning distribution into the other.

With these possibilities, the following scenarios were studied:

1. Wavelet coefficients with Euclidian distance
2. Wavelet coefficients with Euclidian distance calculated independently at each scale
3. Sum of squared wavelet coefficients at each scale with Euclidian distance
4. Relative sum of squared wavelet coefficients at each scale
5. Periodogram with Euclidian distance
6. Periodogram with earth mover's distance
7. Condensed periodogram with Euclidian distance
8. Condensed periodogram with earth mover's distance.

3.2 Discrete Wavelet Transform

The discrete wavelet transform (DWT) of a signal represented by a function $f(x)$ is obtained by applying dilations and translations of a mother wavelet $\psi(x)$ to the function at different scales. For a mother wavelet $\psi(x)$ defined on [0,1], the translation and dilation is obtained as:

$$\psi_{j,k}(x) = 2^{j/2}\psi(2^j x - k).$$

The *wavelet coefficients*, $d_{j,k}$, are calculated as:

$$\mathrm{d_{j,k}} = \int_{-\infty}^{\infty} \mathrm{f(x)}\psi_{\mathrm{j,k}}(\mathrm{x})\mathrm{dx}$$

and can be transformed to obtain the original signal by inverse transform:

$$f(x) = \sum_{j=-\infty}^{\infty} \sum_{k=-\infty}^{\infty} d_{j,k}\psi_{j,k}(x).$$

For a discrete sample $x_1, \dots, x_n$ of length $n = 2^m$ for some m, we can compute the $n-1$ DWT coefficients $d_{j,k}, j = 0, \dots, m, k = 0, \dots, 2^j$. Here, the j subscript corresponds to a *scale* level, with $j = 0$ corresponding to low-frequency. As j increases, the resolution of the coefficients increases through the scaling and dilation of the mother wavelet. So for a series of length $n = 8$, a wavelet decomposition would consist of coefficients $d_{0,0}$, $d_{1,0}$, $d_{1,1}$, $d_{2,0}$, $d_{2,1}$, $d_{2,2}, d_{2,3}$.

For our 2-hour samples of frequency regulation data, we applied the discrete wavelet transform to obtain the wavelet coefficients shown in Figure 3.1. To apply the DWT, we first subsampled our data

down to $2^{10} = 1024$ observations from 1800. This downscaling did not lead to any significant loss of information in the signal. The y-axis in the plot corresponds to the scale level, and as the scale level increases, we get better time resolution. The y-axis labeling on the right of the plot is a translated scale to the corresponding periodicity in minutes. As can be seen, at high scale levels, the coefficients are very small. These coefficients correspond to very high-frequency behavior in the data—what we can think of as noise on top of the signal.

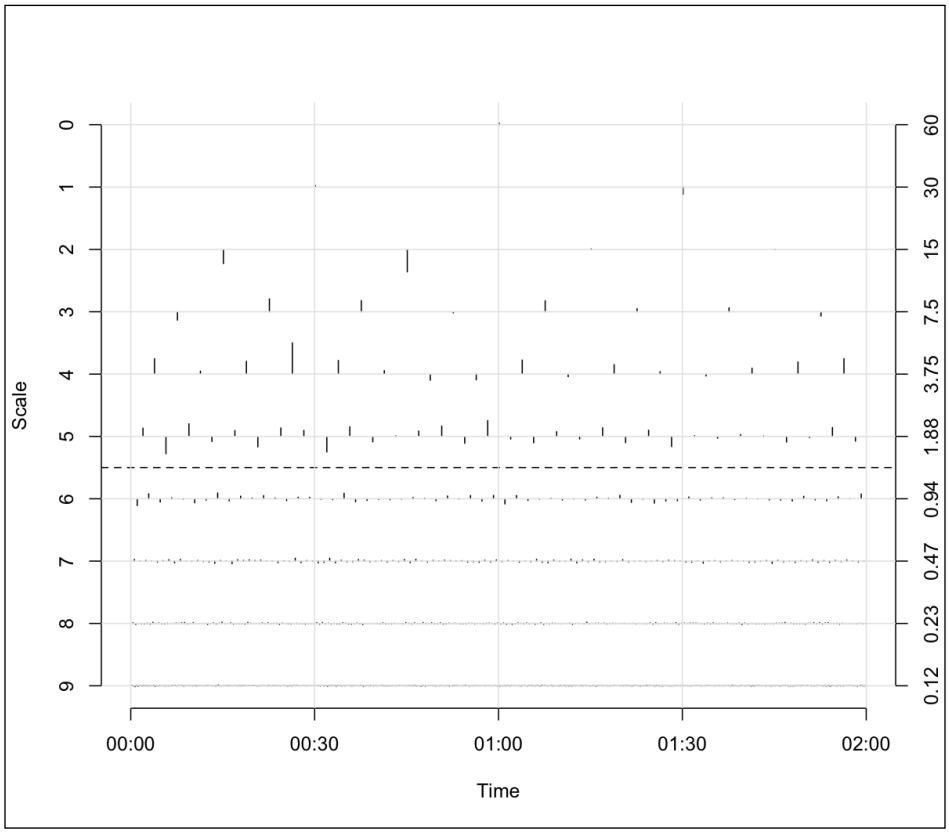

Figure 3.1. Discrete Wavelet Transform for a 2-Hour Period of Frequency Regulation Data

To greatly reduce the dimensionality of the series, we can eliminate these high-frequency coefficients altogether. We keep only the 63 coefficients at scale 5 and above (delineated by the dashed line in Figure 3.1). The condensed set of coefficients represents a smoothed version of the series that still retains the salient features. A plot of the inverse DWT of the thresholded coefficients compared to the original series is shown in Figure 3.2. For more on the DWT and thresholding methods, see [10].

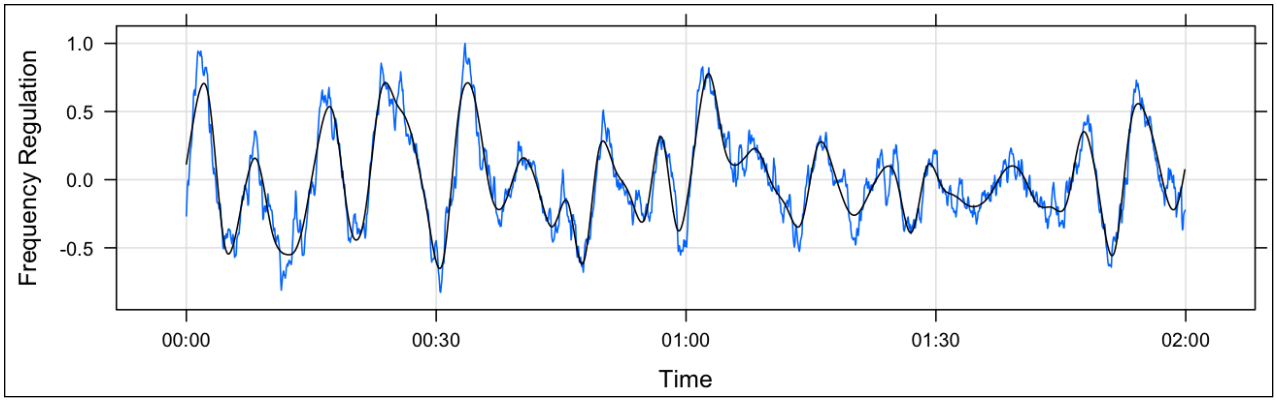

Figure 3.2. Original Frequency Regulation Data with Inverse DWT of Threshold Coefficients

The DWT has given us a useful feature vector for the series in that it reduces the dimensionality of our feature space and also in that it provides measures of activity at different time and frequency scales.

This appears to be a reasonably good approximation to the original signal. The actual peak power is at times 30 percent higher than the approximated power using the inverse DWT coefficients (for example, the first peak after 00:30), with the actual power remaining above the approximated power for about 3 minutes. It should be noted that the peak power is needed for only a few seconds. Hence, to appropriately determine the amount of energy storage needed, the desired surge power (few seconds) needs to be scaled up by 30 percent, while 15 percent higher power needs to be delivered over a 1.5-minute window. Because PHEV batteries typically have a P/E ratio in the range of 10 to 20, this does not appear to be a major roadblock. The additional power could impose incremental stress on the batteries or require more batteries to be available for regulation. With adequate thermal management, thermal stresses on batteries can be minimized.

While this analysis has assumed that the internal resistance of the batteries is not a function of SOC, in actuality, the battery internal resistance increases with decreases in SOC. Also, the rate at which charge can be absorbed decreases with increases in SOC. The PHEV battery test protocol [5] provides some information on estimating available power from the battery SOC for both charge and discharge. Incorporation of this approach would appear to accentuate the importance of the pulse power in Figure 3.2 in order to appropriately determine the minimum number of batteries that need to be available for regulation.

3.3 Wavelet Coefficients by Scale

We also considered clustering based on the total energy at each scale for each sample, using the absolute contribution and relative contribution of the energy at each scale. Let $\mathbf{d}_j = (d_{j,0}, \ldots, d_{j,2^j}), j = 1, \ldots, m$ denote the collection of coefficients at each scale. Then we can calculate the absolute contribution to the total energy at each scale as:

$$e_j = ||\mathbf{d}_j||^2,$$

giving us a total of m features. Likewise, we can compute the relative contribution of each scale on the total as:

$$r_j = \frac{e_j}{\sum_{i=0}^{m} e_i}$$

This normalizes by total energy so that comparisons from one sample to another are not dependent on total energy being different for a given sample. This approach was studied in [1] where they were clustering similar daily load patterns.

3.4 Periodogram Features

Another feature vector we investigated is the periodogram, which is discussed in Section 2.5. The idea of using the periodogram is similar to that of the wavelet coefficients by scale, in that we are aggregating over time and looking at contributions to the total energy at each periodicity. The periodogram values were normalized on the average periodogram over the whole data set. Also, to reduce dimensionality, we studied a condensed version of the periodogram in which frequencies close to each other are merged. This reduction was done in hope of getting more interpretable results.

3.5 Choosing the Number of Clusters

There is a great deal of literature that focuses on choosing the number of clusters. One way is to look at a plot of the within cluster sum of square for various values of K. As the correct choice is approached, the sum of squares should have been reduced significantly by reaching K and then taper off slowly thereafter. Figure 3.3 shows the within cluster sum of squares for each scenario. None of the plots shows any "sweet spot," and we wonder if there are simply too many patterns to get a good clustering with small K values.

Another useful metric for evaluating the number of clusters is the *shadow* value (similar to the silhouette value) [8]. The shadow value is a measure of how separated the clusters are and is defined for a given point as twice the distance to the closest centroid divided by the sum of distances to the closest and second-closest centroids. If the shadow values of a point is close to zero, the point is close to its cluster centroid. If the shadow value is close to 1, it is almost equidistant to the two centroids. Thus, a cluster that is well separated from all other clusters should have many points with small shadow values. We do not include a plot of shadow values here for each cluster, but all scenarios tested had shadow values close to one, which is not a good indication.

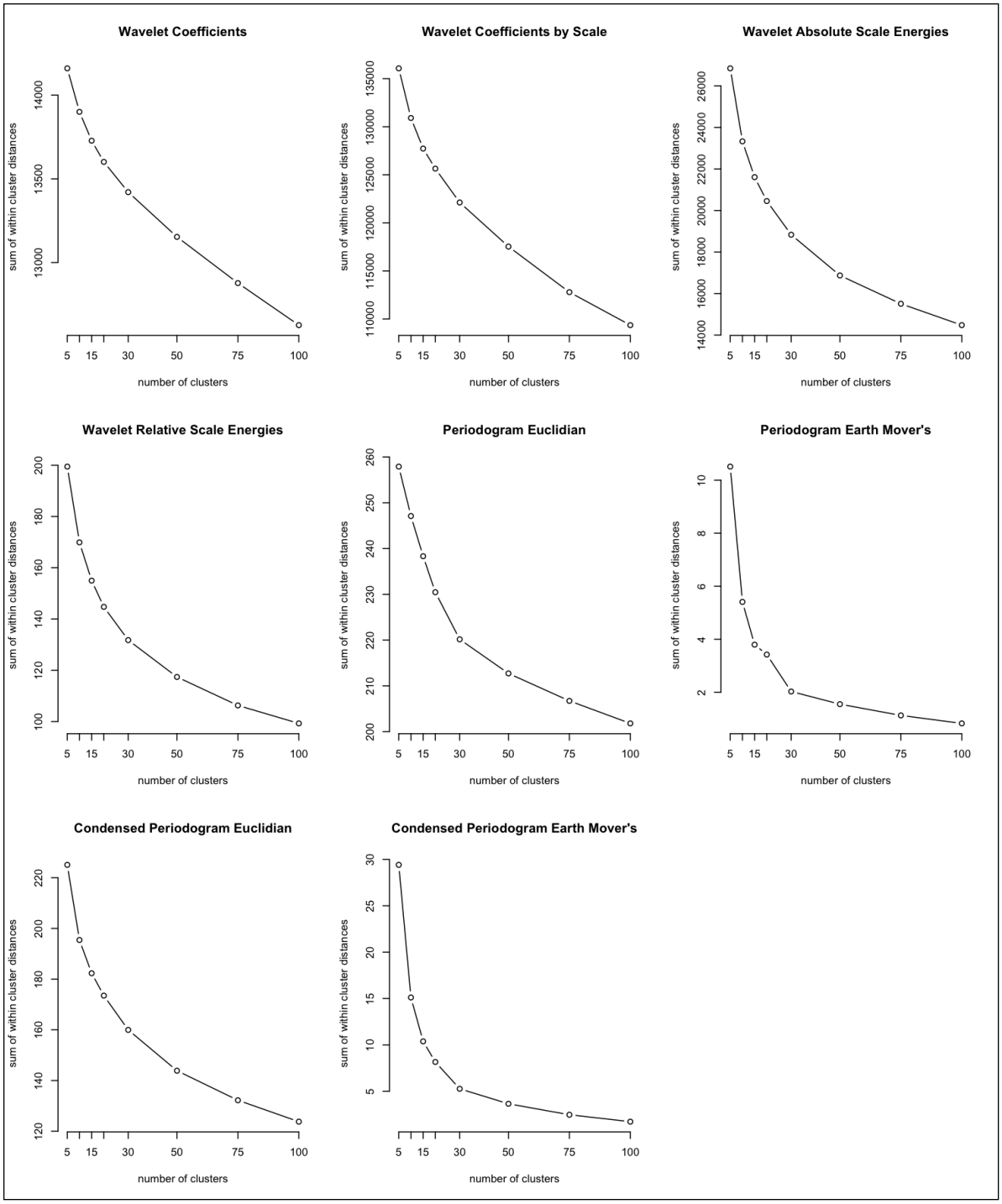

Figure 3.3. Cluster Sums of Squares for Different Choices of *K*

3.6 Evaluating Cluster Results

In the interest of space, we only present results for the clustering approach that we deemed to have the most interesting results. We report on Scenario 1, which used 63 wavelet coefficients as the feature vector for each sample. We visualized some of the results using the flexclust R package [7].

Figure 3.4 shows an image plot of the centroids projected into two dimensions using principal component analysis, with the labels corresponding to each cluster centroid. This helps see how well clusters are separated.

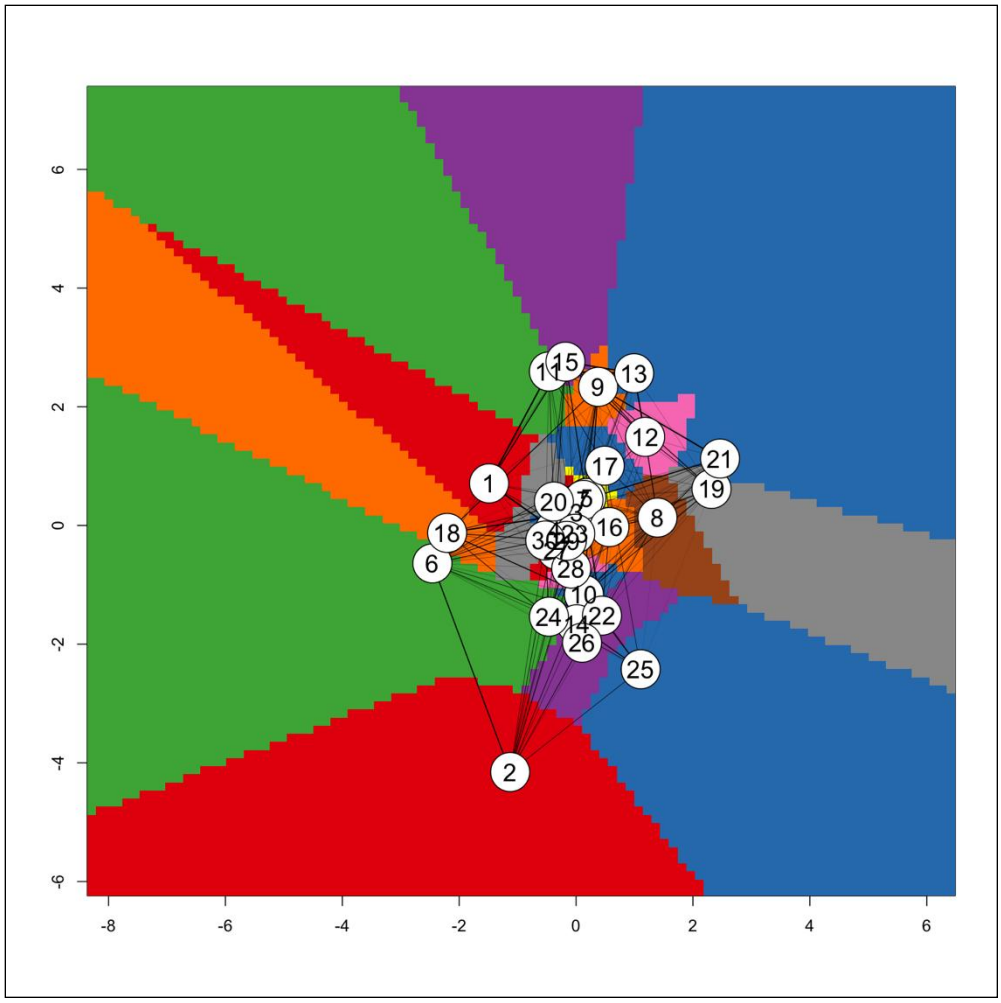

Figure 3.4. Image Plot of Cluster Segments Overlaid by Neighborhood Graph of Wavelet Coefficient Clustering

From Figure 3.4, we see that clusters such as 6, and 15, and 19 are far from each other. We plotted wavelet coefficients corresponding to these three clusters to get an indication of how these three clusters differ. Figure 3.5 shows this plot.

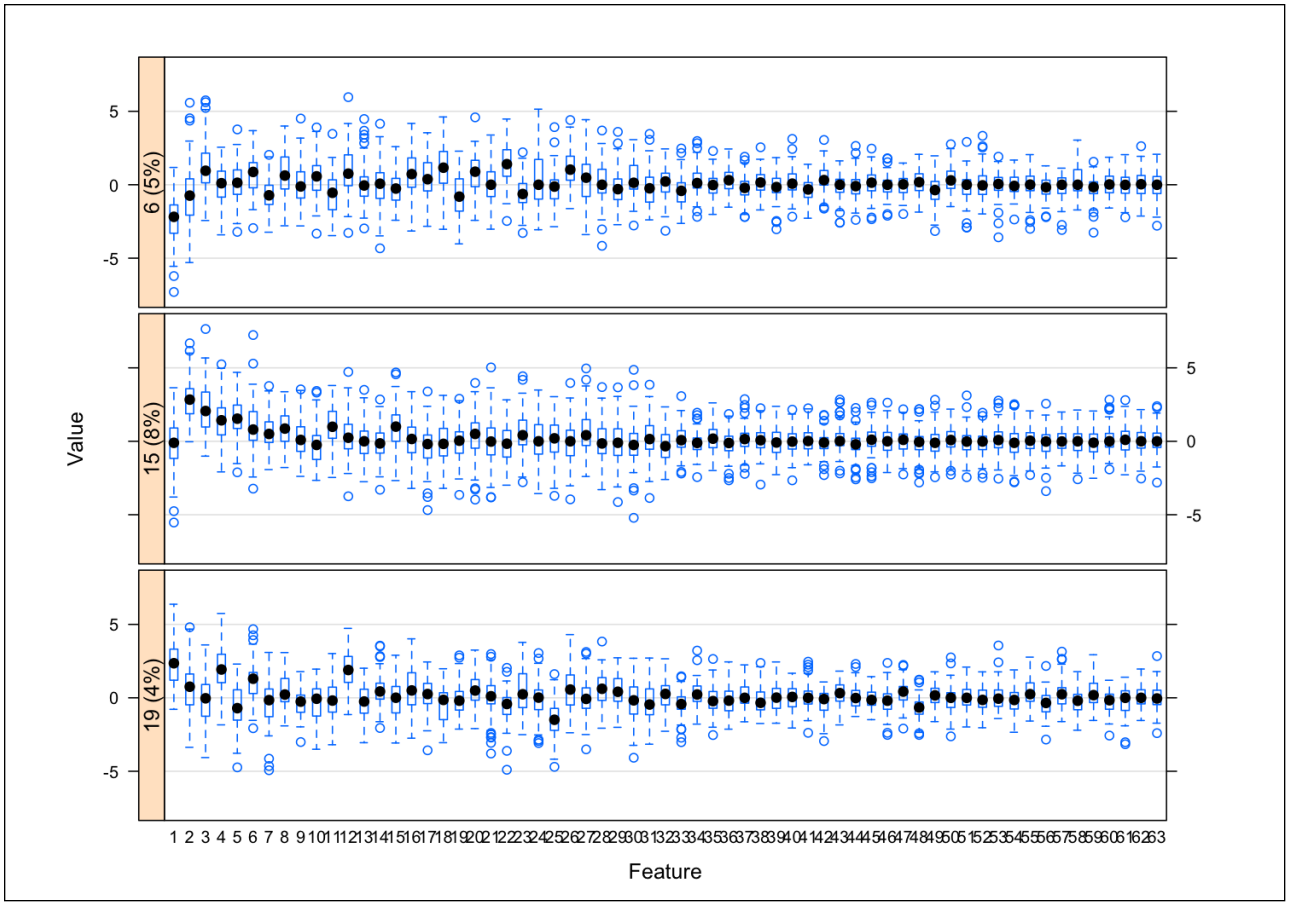

Figure 3.5. Boxplot of Coefficients within Clusters 6, 15, and 19

The x-axis of Figure 3.5 corresponds to each wavelet coefficient, ranging from low frequency to high frequency. The panel labeling indicates the cluster number and the percentage of observations in that cluster. As can be seen, it is mainly the very-low-frequency components that are driving the separation into different clusters. This indicates further reason to first investigate the lower frequency patterns, as done in Section 2.6, and then look for patterns in the remaining higher frequency part of the signal.

A useful way to visualize the clusters is to show each series in each cluster with the centroid overplotted. Figure 3.6 shows this approach, with the red line representing the centroid. This plot also confrims the fact that mainly the low-frequency behavior dominates the differentiation between clusters.

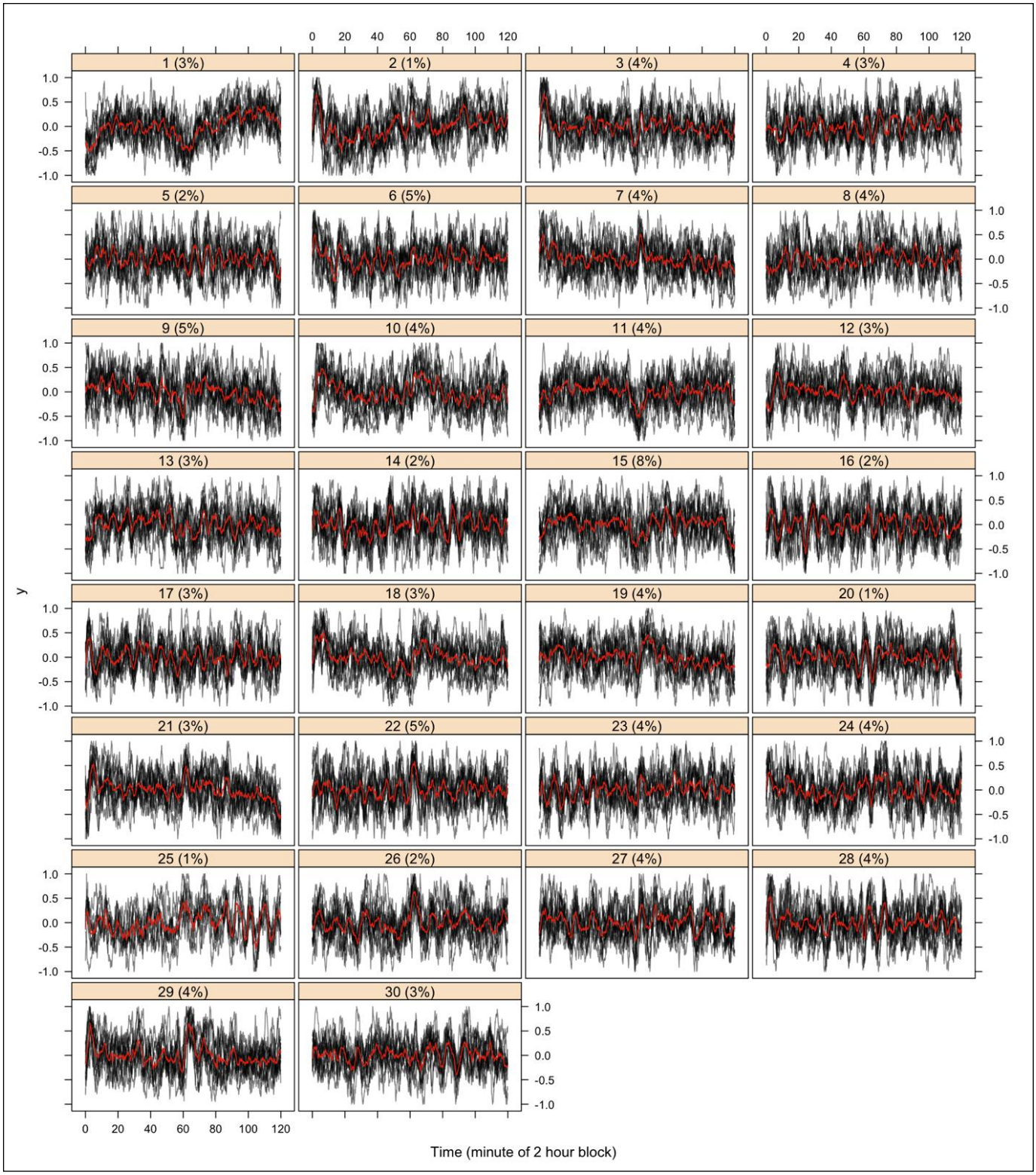

Figure 3.6. All Series in Each of the 30 Cluster Signals Overplotted

The overall directonality of the signal appears to be different for cluster 1 and cluster 7 in Figure 3.6, with the regulation going from negative to positive in cluster 1 and from positive to negative in cluster 7. From Figure 3.7, it is seen that cluster 1 events occur mostly at 20:00 from March 14 to April 18, with the cluster occuring from 12:00 to 16:00 from May 9 to August 1.

Cluster 10 shows a representative low-frequency duty cycle. This candidate would perform a larger 1-hour discharge-charge cycle superimposed by a higher-frequency cycling. The net energy charged and discharged for the 2-hour duration would be approximately zero. However, the depth of discharge for each half cycle is quite high; thus, the battery cycle life would be directly impacted. This would mean that the starting and ending SOC would be identical. This particular testing cycle candidate would lend itself to be repeated multiple times without any further charge corrections.

The other key point is that cluster 17 is power intensive, with the power oscillating with a period of 8 minutes. While cluster 1 has a dominant low-frequency behavior with a period of 60 minutes. By determining the actual power scale for these clusters, one can develop a boundary condidtion for energy- and power-related strains the PHEV batteries will be subjected to during the course of a year. The energy related-strain would be the imposition of sequentially lower or higher SOC at the end of each hour for cluster 1 or cluster 7. The power-related strain would be the imposition of discharge pulses at a low SOC and charge pulses at a high SOC, especially at low ambient temperatures.

Figure 3.7 shows the clustering results by time-of-day and across time-of-year. The purpose of this figure is to highlight whether observations within clusters tend to occur at the same time-of-day or time-of-year. Each panel corresponds to a cluster, and if a colored box is present, this means that there is an observation in that cluster that occurred on that day at that time. The different colors aid in distinguishing between time-of-day. Certain clusters, such as cluster 10, have behavior restricted to only the midnight hours. Based on our analysis in Section 2.6, this is actually not surprising in that we saw that there are distinct within-hour behaviors at these hours.

As discussed earlier, the net charge and net discharge patterns can be readily addressed by adjusting the battery SOC to levels that would prevent the SOC from crossing the lower and upper limits of 20 and 80 percent, respectively.

It should be noted that this analysis does not account for the fact that the charging rate for lithium-ion batteries has restrictions. However, it can be assumed that this restriction applies for long-term continuous charging, while pulses at the 20C rate for a few seconds can be sustained. Charging rate should be limited to low rates (<1C) at low temperatures (<4ºC). Assuming that most of the batteries will be stored in garages and assuming that garage temperatures are generally above 4ºC, it is safe to assume that battery temperatures would be >4ºC during regulation service.

The effect of the duty cycle on battery life can be estimated from readily available curves that relate battery cycle life to depth of discharge. Data on battery calendar life can be used to further estimate the state of health (SOH) of a battery as it ages. A further consideration of the thermal stresses that batteries are subjected to during pulse charging/discharging would provide additional information on battery SOH during operation. A comprehensive tool that estimates battery SOH by combining the effects of its drive cycle with the duty cycle during regulation needs to be developed.

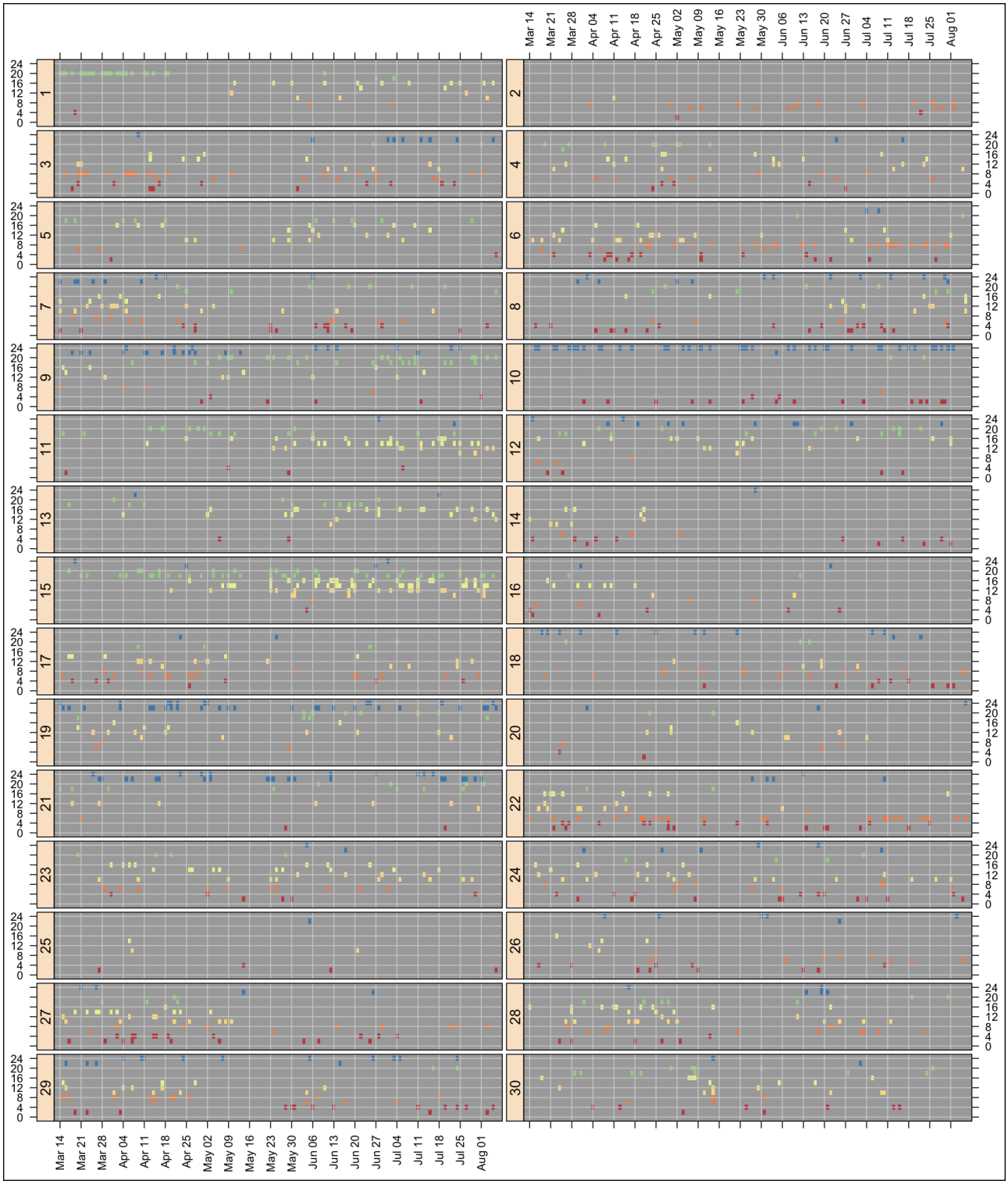

Figure 3.7. Time-of-Day Plot

3.7 Choosing a Representative Signal

A major finding from the exploratory and cluster analysis is that, although there are many systematic properties of the frequency regulation signal, there are still many distinct patterns in the data with no clear emergence on a few representative patterns. Given the existing data set, this outcome necessatates the use of other corroborating information or insights from a battery-testing perspective that will reduce the set of potential patterns to a managable number.

To narrow down the number of drive cycles, we applied perspectives accounted for battery SOH.. There are three disctinct patterns out of the 30 clusters that would impose fundamentally different testing regimes for batteries. These patterns are described below:

1. *Curves with directionality and sign of the signal changing from positive to negative or vice versa*. Cluster 1 is an example of positive directionality

2. *Low-frequency signal*. Cluster 10 shows a representative duty cycle. This candidate would perform a larger 1-hour discharge/charge cycle superimposed by higher-frequency cycling. The net energy charged and discharged for the 2-hour duration would be approximately zero. This would mean that the starting and ending SOC would be identical. This particular testing cycle candidate would lend itself to be repeated multiple times without any further charge corrections.

3. *High-frequency signals superimposed on each other and curves with signals that oscillate symmetrically around zero*. This case is quite straightforward and ideal for batteries. Cluster 17 shows a representative duty cycle with these characteristics. The net energy exchange also is approximately zero. However, different from the low-frequency signal is that the variation in the SOC domain is much less than for the low-frequency cycle. The high-frequency cycle stresses the battery more as a power provider with less energy capacity required.

4.0 Conclusions and Future Work

This analysis explored methods for characterizing the time series of regulation signals with the objective of developing characteristic cycles for batteries used as regulation providers. We used exploratory analysis and cluster analysis based on wavelet coefficients to identify distinctive signals. We feel that the results from this work will be useful in follow-up studies of battery stress tests.

4.1 Exploratory analysis results

The spectral analysis revealed patterns in the regulation signal with distinct periodicities in the 1-hour, 30-minute, and 7.5-minute cycles. We believe the periodicities reflect the specific PJM market design.

Observed differences as a function of time-of-day are summarized below:

- *Mean value of regulation.* There is a propensity for the mean of the regulation signal to be slightly biased above zero during the middle of the day (06:01 to 18:00) and slightly biased below zero in the night hours (18:01 to 06:00). This propensity has important implications to batteries in that, unless otherwise compensated, on average there would be a net charging of a battery plugged in during the night and, conversely, a net discharging during the day. Net charging during the night for plug-in electric vehicles can be accommodated easily without any compensation, but net discharging during the day will need to be compensated so the vehicle battery can be recharged for the next drive.

- *Amplitude of regulation cycling*. The amplitude swing (i.e., the minimum-maximum spread) of the cycles in the regulation signal has a propensity to be higher during the night and lower during the day. In fact, we found that a significant relationship exists between the system load level and the amplitude of the regulation signal. Under low-load conditions, the amplitude of regulation grows exponentially compared to the amplitude at high-load conditions. This means that, during the day, either fewer vehicle resources are necessary to meet the regulation requirements or, if the resource availability is held constant during the 24-hour day (i.e., the same number of vehicles offer the same service for 24 hours), the individual contribution by each vehicle is less during the day than at night. As a consequence, the amplitude for defining the performance test or drive cycle potentially could be smaller during the day than at night.

Similarly, we found seasonal differences that would scale with the month of the year. Exploring the range of low-frequency (1-hour cycles) to high-frequency (7.5-minute cycle) signals across all seasons indicates that the lower frequency component in the regulation signal increases in significance from the winter to summer months. The mid-range (30-minute cycles) remains constant across the month studies, while the lower frequency components (7-minute cycles) slightly decrease their contribution to the overall signal for the period from March through August. Low-frequency cycles require more energy capacity than do high-frequency cycles. Low-frequency cycles with higher energy requirements cause large cycles across the SOC scale for any given battery size. For transportation batteries, this means higher burden on the remaining life of the battery as it may encounter deeper depths of discharge over any given period of time than would occur if it were exposed to higher frequency regulation signals.

4.2 Cluster Analysis

The statistical clustering approach used in this study reflected the large diversity in patterns of the regulation signal and resulted in rather large number of clusters to characterize the entire data set. As a consequence, the prospect of finding a small number of representative cycles using the clustering approach does not seem to be promising. Additional information grounded in an understanding of battery testing procedures must inform the selection process.

The results distinguished clusters of similar behavior based on dominant low-frequency cycles (i.e., 30-minute to 1-hour cycles). Cycles in the same cluster have similar time-of-day properties, indicating that similar patterns occur in many cases at the same time of the day.

The regulation signals revealed system behaviors of PJM's market structure. The 1-hour cycle components of the regulation signal is a clear reflection of hourly markets causing a rearrangement of generators participating in the day-ahead hourly energy market. The dependency of the regulation signal on the frequency and timing of market clearings suggests that the results are strictly valid for the current PJM wholesale markets. As PJM's market design changes, it is very likely that the key oscillatory content will change as well. With the general trend in the competitive wholesale market to clear in shorter and shorter time periods, there could be a propensity for regulation signals to increase the shorter cycles. Furthermore, the integration of an increasing capacity of intermittent wind and solar resources will very likely introduce new dynamics to the regulation requirements caused by the varying output of the wind and solar installations. How the growing wind and solar capacity may influence the regulation signal is unclear. Weather phenomena and the diversity of the wind and solar insolation across a balancing area will impact the regulation signal. Furthermore, the change in the generation inertia by the growing wind and solar generation resources also may influence the dynamics of the power system and, in turn, impact the regulation signal.

4.3 Recommendations for Selection of V2G Drive Cycles

From the cluster analysis, it is clear that some clusters are dominated by high frequency (a period of 10 minutes), while other clusters are dominated by low frequency (a period of 60 minutes). These can easily establish an upper boundary condition on the power- and energy-related strain the battery is subjected to during regulation throughout the year.

Despite the large diversity of low- and high-frequency characteristics across the time scale in the PJM data set, we do offer some recommendations for the selection of potential candidates for testing cycles that are informed by battery experts. The recommendations are based on both the findings of the cluster analysis and are further informed by an understanding of battery degradation mechanisms and battery performance testing. Across the diversity of 30 distinct clusters, a set of duty cycles from three particular clusters are recommended as potential candidates for future standards development. These three clusters are summarized below:

1. *Curves with directionality and sign of the signal changing from positive to negative or vice versa*. Cluster 1 is an example of positive directionality. Further studies will focus on the number of back-to-back clusters with the same directional trend to estimate the ability of the batteries to

keep their SOCs within the desired range, and the ability of the batteries to provide the desired power for the required amount of time.

2. *Low-frequency signal*. Cluster 10 shows a representative duty cycle. This candidate would perform a larger 1-hour discharge/charge cycle superimposed by higher-frequency cycling. The net energy charged and discharged for the 2-hour duration would be approximately zero. This would mean that the starting and ending SOC would be identical. This particular testing cycle candidate would lend itself to be repeated multiple times without any further charge corrections.

3. *High-frequency signals superimposed on each other and curves with signals that oscillate symmetrically around zero*. This case is quite straightforward and ideal for batteries. Cluster 17 shows a representative duty cycle with these characteristics. The net energy exchange also is approximately zero.

A preliminary conclusion of this work is that, by appropriate energy management, a single protocol can be developed for performance testing of PHEV batteries by simulating their drive cycle and frequency regulation.

4.4 Next Steps Toward Standardizing V2G Drive Cycles

This analysis is the first of several steps toward standardizing V2G drive cycles or battery testing cycles. The next step is to perform a similar exploratory analysis with regulation data sets from other regions of the United States to explore potential regional differences that reflect different market designs, system responses, and system characteristics. After these regional studies, the results can be discussed from a national perspective to identify a set of characteristics that are sufficiently representative for the U.S. grid.

It is anticipated that the statitistical analyses will provide the necessary bachground information to formulate a set of test procedure proposals. With continuing support for this analysis, it is reasonable to expect statistical analysis for the entire United States can be completed toward the end of the FY 2012, with standards discussions possibly commencing in the fall and winter of 2012. The appropriate standards body could be the Institute of Electrical and Electronics Engineer (IEEE).

5.0 References

[1] Antoniadis, A. and Brossat, X. and Cugliari, J. and Poggi, J.M. Clustering functional data using wavelets. 2011.

[2] Cleveland, W.S. and Devlin, S.J. and Grosse, E. Regression by local fitting: Methods, properties, and computational algorithms. *Journal of Econometrics*, 37(1):87--114, 1988.

[3] Cryer, J. and Chan, K. *Time series analysis with applications in R.* Springer, 2008.

[4] EPA, 1993. Federal Test Procedure Review Project: Technical Report. May 1993. EPA 420-R-93-007. Certification Division, Office of Mobile Sources. U.S. Environmental Protection Agency. Washington D.C.

[4] Goldin, D. and Mardales, R. and Nagy, G. In search of meaning for time series subsequence clustering: matching algorithms based on a new distance measure. *Proceedings of the 15th ACM international conference on information and knowledge management*, pages 347--356, 2006. ACM.

[5] Idaho National Laboratory, Battery Test Manual for Plug-In Hybrid Electric Vehicles Revision 1, September 2010.

[6] Kirby, B.J. *Frequency Regulation Basics and Trends*, December 2004

[7] Leisch, F. A toolbox for k-centroids cluster analysis. *Computational statistics & data analysis*, 51(2):526--544, 2006.

[8] Leisch, F. Neighborhood graphs, stripes and shadow plots for cluster visualization. *Statistics and Computing*, 20(4):457--469, 2010.

[9] Ling, Haibin and Okada, K. An efficient earth mover's distance algorithm for robust histogram comparison. *IEEE Transactions on Pattern Analysis and Machine Intelligence*, 29(5):840-53, 2007.

[10] Nason, G.P. *Wavelet methods in statistics with R*. Springer Verlag, 2008.

[11] R Development Core Team. *R: A Language and Environment for Statistical Computing*. R Foundation for Statistical Computing, Vienna, Austria, 2011. ISBN 3-900051-07-0.

Distribution

No. of
Copies

Name
Organization
Address
City, State and ZIP Code

Organization
Address
City, State and ZIP Code
Name
Name
Name
Name
Name (#)

Name
Organization
Address
City, State and ZIP Code

No. of
Copies

 # Foreign Distribution

Name
Organization
Address
Address line 2
COUNTRY

 # Local Distribution

Pacific Northwest National Laboratory

Name	Mailstop
Name	Mailstop
Name	Mailstop
Name	Mailstop
Name	(PDF)

Pacific Northwest
NATIONAL LABORATORY

U.S. DEPARTMENT OF
ENERGY

Proudly Operated by Battelle *Since 1965*

902 Battelle Boulevard
P.O. Box 999
Richland, WA 99352
1-888-375-PNNL (7665)
www.pnl.gov